Åbo Akademi University

RAMAKRISHNA JOGI

Green aviation fuel hydrocarbons from lignocellulosic biomass via hydrothermal liquefaction

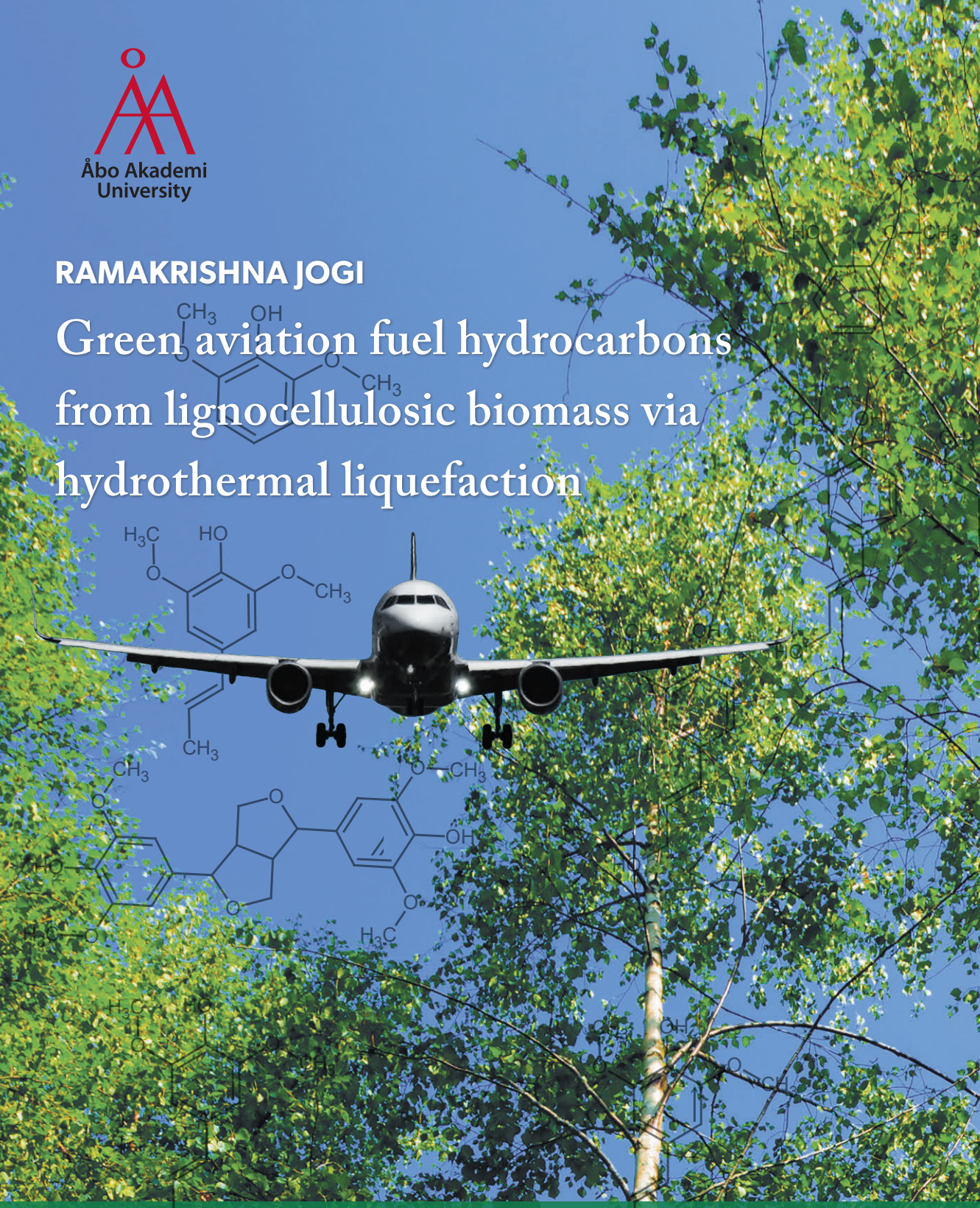

Laboratory of Industrial Chemistry and Reaction Engineering
Faculty of Science and Engineering / Chemical Engineering
Åbo Akademi University
Turku/Åbo 2021

Ramakrishna Jogi

Born 1988, Narasapur-534275, INDIA
M.Sc. Analytical Chemistry 2010
GITAM Institute of Science
GITAM University-530045, INDIA

Green aviation fuel hydrocarbons from lignocellulosic biomass *via* hydrothermal liquefaction

Ramakrishna Jogi

Doctoral Dissertation

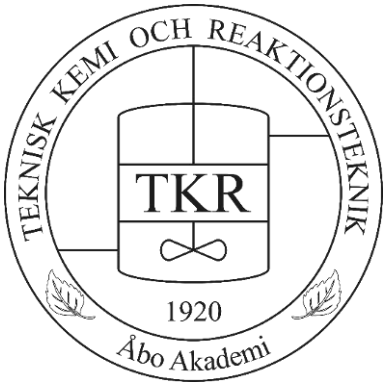

Johan Gadolin

Process Chemistry Centre

Laboratory of Industrial Chemistry and Reaction Engineering
Faculty of Science and Engineering/Chemical Engineering
Åbo Akademi University
Turku/Åbo, Finland, 2021

Supervised by

Professor Jyri-Pekka Mikkola
Laboratory of Industrial Chemistry and Reaction Engineering
Johan Gadolin Process Chemistry Centre
Åbo Akademi University
Åbo/Turku, Finland & Umeå University, Sweden

Associate Professor Päivi Mäki-Arvela
Laboratory of Industrial Chemistry and Reaction Engineering
Johan Gadolin Process Chemistry Centre
Åbo Akademi University
Åbo/Turku, Finland

Docent Pasi Virtanen
Laboratory of Industrial Chemistry and Reaction Engineering
Johan Gadolin Process Chemistry Centre
Åbo Akademi University
Åbo/Turku, Finland

Reviewers

Professor Knut Irgum
Department of Chemistry
Umeå University
Umeå, Sweden

Docent Ikenna Anugwom
LUT University Lappeenranta Campus
School of Engineering Science
Lappeenranta, Finland

Faculty opponent

Professor Knut Irgum
Department of Chemistry
Umeå University
Umeå, Sweden

ISBN 978-952-12-4039-3 (printed version)/ ISBN 978-952-12-4040-9 (digital version)
ISSN 2669-8315 2670-0638 (*Acta technologiae chemicae Aboensia 2019 A/1*)
Painosalama Oy Åbo/Turku 2021

“నా ఉనికికి కారణభూతులైన మీకు ఏమివ్వగలను, నేను పొందిన
జ్ఞాన కుసుమాలను తప్ప...”

This thesis is dedicated to my parents.

For their endless love, support and encouragement

My brother says all the time
-"where there is the will-there is the way"

I truly believe in it

Preface

When I look back on my earlier days, I am still surprised and do not have words to express my feelings on paper. It is a big miracle in my life to be in Finland from India. Years later, I still remember to feel as thankful and wondered as I was arriving on the first day at midnight (01:00 Am on 21-08-2017), maybe even more. I have learned so much from the people of Finland; especially the city of Turku (Åbo in Swedish) people are very practical, punctual, and polite (can be termed as P^3). These characters changed my lifestyle, for the rest of my life, I am thankful to them. The completion of this doctoral study provided me with an opportunity to express thanks to many people in my journey.

I would like to express profound gratitude to Professor Jyri-Pekka Mikkola, who has introduced me to building of a sustainable world for the future generation and for the opportunity to try new things for me like 'hydrothermal liquefaction, deep eutectic solvents, and aviation fuel range hydrocarbons', and also for sharing his scientific passion and experiences. I would like to express my deepest gratitude to Associate Professor Päivi Mäki-Arvela, and Docent Pasi Virtanen, who were providing valuable bits of advice, energetic participation in experiments, and supervision in everyday research work. The completion of doctoral study would not have been possible without Päivi's and Pasi's support. I irritated them many times with different research questions, but they break it with a little smile. I never met such people in my life; would like to say they are the best example of P^3. I am also grateful to Academy Professor Tapio Salmi for the chance to work in such a vivid and dynamic laboratory. I would like to thank Professor Dmitry Murzin as well for always offering the very best scientific discussions and inspiring lectures. Prof. Dmitry is an example of high-level research and lectures. I would like to thanks Professor Henrik Grénman and Professor Johan Wärnå for their inspirational discussions and lectures. I would like to acknowledge Docent Narendra Kumar, who provided his support for the preparation of catalysts, characterizations, and being so kind. I would like to express appreciation to Docent Kari Eranen for his support with instrumentation and chemicals.

Special thanks to all co-authors in my publications: Prof. Chunlin Xu, Docent Narendra Kumar, Jarl Hemming, Annika Smeds (ÅAU); Dr. Ajaikumar Samikannu, Dr. Santosh Govind Khokarale and Dr. Chandrakant Mukesh (Umeå University); Dr. Torbjörn A Lestander (Swedish University of Agricultural Sciences); Prof. Krisztian Kordas, Dr. Aron Dombovari (University of Oulu); Assistant Professor Vincenzo Russo (University of Naples Federico).

With best regards, I would like to thank all colleagues and friends at the laboratory for the nice working atmosphere, Nemanja, Adriana, Pasi Tolvanen, Wander, Erfan, Lu, Ekaterina, Soudabeh, Atte, Ole, Matias, Maria, Jussi, Zuzana, Ananias, Mouad, Christopher, Mark, Moldir, Anton, Lidia, Imane, Thank you.

I am also using this opportunity to express sincere appreciation to my parents, Mrs. Peddintlu Jogi (mom) and Mr. Adhrusta Rao Jogi (dad). Everything I am today is because of them. My deepest gratitude to mom, not only mom, she is my best friend ever in my life, who she is with me in all test times and strengthens. Besides, thanks to my elder brothers (Konda and Ravi), relatives, and the dearest friends Easwar and Venkatesh's encouragement.

Finally yet importantly, about my family. When I have arrived in Finland with a single status, then after one year a beautiful woman entered into my life, Jyothsna Devi (wife) changed single status, broke the loneliness, and filled with happiness. I am very grateful to have your support at all times, thank you darling Joshi. At the time of thesis writing, a newcomer entered into my life and made vibrant with her smile, my daughter Bhuvisri Aadhya, you are the reason to finish thesis writing without any tensions. Thank you ra Bhuvi talli for your love and everything.

Abstract (in English)

Green aviation fuel hydrocarbons from lignocellulosic biomass *via* hydrothermal liquefaction

-Ramakrishna Jogi

Hydrothermal liquefaction (HTL) of lignocellulosic biomass in primary alcohols is a novel thermochemical method to produce sustainable aviation fuel range cyclic hydrocarbons. In this method, particularly the underutilized wood fractions, hemicellulose and lignin components are dissolved to produce biocrude. The current planned process comprises of three phases, such as production of biocrude through HTL, extraction of bio-aromatics from biocrude using deep eutectic solvents (DES) and further transformation of bio-aromatics into cyclic hydrocarbons *via* hydrodeoxygenation (HDO). The main aim of this work was to utilize the heterogeneous catalysts in HTL method to produce biocrude at fixed temperature and under low initial hydrogen pressure in supercritical ethanol. The selection of catalysts was based on the acidity of the support material and transition metal immobilized on the support. The following catalysts were applied: 5 wt. % Fe-Beta-150 exhibiting with weak and medium Brønsted-Lewis acidity or non-acidic 5 wt. % Fe-SiO_2 and weakly Brønsted acidic $NbOPO_4$ or Pd/$NbOPO_4$ with weak Lewis acidity.

In-house prepared and characterized Fe-based catalysts were used in birch fractionation. The influence of gaseous atmosphere and catalyst acidity as well as formation of phenolic products during liquefaction was studied over 5 wt. % Fe-H-Beta-150 or 5 wt. % Fe-SiO_2. After the experiments, the liquid, solid and gaseous products were fully characterized using several analytical techniques. The obtained results show that Brønsted-Lewis acidic 5 wt. % Fe-H-Beta-150 catalyst, gave rise to around 25 wt. % of biocrude with 68 wt. % aromatic products, while non-acidic 5 wt. % Fe-SiO_2 catalyst only gave around 18 wt. % of biocrude with 38 wt. % aromatic products. A Brønsted acidic catalyst enhances the dissolution efficiency, particularly hemicellulose and lignin degradation into biocrude with increased formation of acids, esters and aromatic compounds. Relatively low amounts of gaseous products were formed and catalyst leaching during liquefaction was low. Based on X-ray diffraction measurements of the solid wood residue, amorphous cellulose part transformed into crystalline state during liquefaction. From the liquid phase analysis results as a function of time, a reaction mechanism was proposed for the lignin degradation products over 5 wt. % Fe-H-Beta-150 or 5 wt. % Fe-SiO_2 catalysts. The main lignin degradation product was isoeugenol, while some other intermediate products, *i.e.* coniferyl, and sinapyl alcohol, 4-propenyl syringol, syringaresinol, along with syringyldehyde rapidly reacted further. To support the proposed reaction mechanism, the thermodynamic analysis was also performed using the Joback approach and Gibbs-Helmholtz equation. In case of Nb-based

catalysts, $Pd/NbOPO_4$ catalyst was prepared through wet-impregnation method and fully characterized. Reaction conditions were optimized and catalytic liquefaction over $Pd/NbOPO_4$ was compared with fresh and acetone extracted birch. In addition, the influence of support, and metal upon the liquefaction of birch were determined. From the liquid phase results, the main product in lignin degradation was homosyringaldehyde, opposite to 5 wt. % Fe-H-Beta-150, for which isoeugenol was the main product contrary to $Pd/NbOPO_4$ catalyzed hydrogenation of sinapyl alcohol to dihydroconiferyl alcohol. The fresh treated wood over $Pd/NbOPO_4$ resulted in the formation of 34 wt. % of phenolic monomers composed of 76.9 wt. % of dimethoxyphenols and 16.5 wt. % of guaiacol related monomers. The liquefaction of acetone extracted birch treated over $Pd/NbOPO_4$ gave 35 wt. % of lignin monomers containing 93.2 wt. % of dimethoxyphenols and 6.8 wt. % of guaiacol based monomers. The delignification efficiency during liquefaction of fresh and acetone-extracted birch over $Pd/NbOPO_4$ was also determined. Based on the liquid phase results the following reaction mechanism was proposed: Lignin degradation occurs *via* cleavage of ether bonds, which is catalyzed by Lewis acid sites in the solid acid catalyst. Thereafter, dehydration/dealkylation of monophenols occurred over Pd metal under low initial hydrogen pressure. Furthermore, a novel extraction method to extract the aromatic fraction from biocrude was developed. A deep eutectic solvent (DES) composed of choline chloride: ethylene glycol (1:4 mol) was used in a step-wise method with methyl isobutyl ketone (MIBK) and water.

Referat (in Swedish)

Gröna flygbränslekolväten genom hydrotermisk förvätskning av lignocellulosisk biomassa

-Ramakrishna Jogi

Termisk behandling av lignocellulosabaserad biomassa under vätgas (engl. Hydrothermal liquefaction (HTL)) i en primär alkohol är en ny metod för framställning av cykliska kolväten som används som komponenter i förnybar flygbränsle. I denna metod framställs ”biocrude” (bioråolja) genom att upplösa underutnyttjade vedkomponenter, d.v.s. hemicellulosa och lignin. Den utvecklade processen består av tre steg, ss. framställning av bioråolja via HTL metoden, extraktion av aromatiska komponenter med hjälp av djupt eutektiska lösningsmedel och deras omvandling till cykliska kolväten via hydrodeoxygenering (HDO). Målsättningen med denna forskning var att utnyttja heterogena katalysatorer genom HTL metoden för framställning av bioråolja vid en viss temperatur under ett lågt vätgas tryck under överkritisk etanol. Katalysatorer valdes på basen av bärarmaterialets surhet och övergångsmetaller immobiliserades på bärarmaterialet. Följande katalysatorer användes: 5 vikt % Fe-Beta-150 som innehåller båda svaga and medelstarka Brønsted och Lewis sura säten, en icke-sur 5 vikt % Fe-SiO_2 med svaga Brønsted sura säten samt sur NbOPO4 eller Pd/$NbOPO_4$ med svag Lewis surhet.

Fe-baserade katalysatorer, som framställdes vid laboratoriet och karakteriserades, användes i björk fraktionering. Inverkan av gasatmosfären inne i reaktor samt katalysatorns surhet undersöktes tillsammans med bildning av fenoliska komponenter i fraktioneringen på 5 vikt % Fe-H-Beta-150 eller 5 vikt % Fe-SiO_2. Efter utföring av experimenten, analyserades vätske, fastfas och gasformiga produkter med olika analysmetoder. Resultaten visade att 25 vikt % biocrude samt 68 vikt % aromatiska produkter kunde produceras på 5 vikt % Fe-H-Beta-150 katalysator som innehöll Brønsted surhet, medan med hjälp av en icke-sur 5 vikt % Fe-SiO_2 katalysator bara 18 vikt % av biocrude innehållande 38 vikt % aromatiska produkter kunde framställas. En katalysator med Brønsted sura säten påskyndade fraktioneringen, eftersom speciellt vid upplösning av hemicellulosa och lignin bildades det syror, estrar samt aromatiska komponenter. Det bildades relativt låga halter av gasfasprodukter och upplösning av katalysator under fraktioneringens förlopp var minimal. Röntgendiffraktionsmätningar av det fasta resterande vedet visade att den amorfa cellulosan hade omvandlats till kristallint under fraktioneringen. Från vätskefasanalyser som funktion av tid föreslogs det en reaktionsmekanism i vilken ligninupplösning i närvaro av 5 vikt % Fe-H-Beta-150 eller 5 vikt % Fe-SiO_2 katalysatorer blev huvudprodukten isoeugenol, medan som andra biprodukter bildades det koniferyl och sinapyl alkohol, 4-propenyl syringol samt syringaresinol. Resultaten visade också att syringyldehyd reagerade snabbt vidare. Den

föreslagna reaktionsmekanismen bekräftades ytterligare genom att utföra en termodynamisk analys med hjälp av Joback metoden och Gibbs-Helmholtz ekvationen. $Pd/NbOPO_4$ framställdes *via* våt-impregneringsmetoden och karakteriserades med olika metoder. Reaktionsbetingelser optimerades i den katalytiska vedfraktioneringen på $Pd/NbOPO_4$ och resultaten jämfördes med de resultaten där acetonextraherat björk användes som råmaterial. På basen av vätskefasanalyser påvisades det att huvudprodukten i lignin upplösning var homosyringaldehyd, i motsats till de resultaten på 5 vikt % Fe-H-Beta-150, där isoeugenol var huvudprodukten. $Pd/NbOPO_4$ katalyserade hydrering av sinapyl alkohol till dihydrokoniferyl alkohol. Behandling av det färska vedet med $Pd/NbOPO_4$ gav 34 vikt % fenoliska monomerer av vilka 76.9 vk. % var dimetoxyfenoler samt 16.5 vikt % guaiakol relaterade monomerer. Fraktionering av aceton-extraherad björk med $Pd/NbOPO_4$ gav 35 vikt % lignin monomerer som innehöll 93.2 vikt. % dimethoxyfenoler och 6.8 vikt % guaiakol baserade monomerer. Fraktioneringseffekten av färsk och acetonextraherad björk på $Pd/NbOPO_4$ undersöktes också. På basen av vätskefasanalyser föreslogs följande reaktionsmekanism: Lignin upplösning sker via nedbrytning av eterbindningar som katalyseras av Lewis syra säten på den fasta katalysatorn. Dekarbonylering, som ett efterföljande steg framskrider på Pd metall under ett lågt vätgastryck. Dehydrering och dealkylering av monofenoliska komponenter sker också på Pd metall under ett lågt vätgastryck. Ytterligare utvecklades det en ny extraktionsmetod för separering av den aromatiska fraktionen from bio-olja. Ett djup eutektiskt lösningsmedel (eng. deep eutectic solvent (DES)) uppbyggd av kolinklorid: etylenglykol (1:4 mol: mol) användes i en stegvis metod i vilken även metyl isobutyl keton (MIBK) och vatten användes som andra lösningsmedel.

క్లుప్త వ్యాఖ్యానం (In Telugu)

లిగ్నో సెల్యులోసిక్ బయోమాస్ నుండి హైడ్రోథర్మల్ ద్రవీకరణ ద్వారా గ్రీన్ ఏవియేషన్ ఇంధన హైడ్రోకార్బన్లు

- రామకృష్ణ జోగి

లిగ్నోసెల్యులోసిక్ బయోమాస్ (lignocellulosic biomass) ను ప్రాధమిక ఆల్కహాల్లలో హైడ్రోథర్మల్ లిక్విఫ్యాక్షన్ (హెచ్టిఎల్) (hydrothermal liquefaction-HTL) పద్ధతి ద్వారా స్థిరమైన విమానయాన ఇంధన శ్రేణి చక్రీయ హైడ్రోకార్బన్లను ఉత్పత్తి చేయటం ఒక గొప్ప థర్మోకెమికల్ పద్ధతి. ఈ పద్ధతిలో, ముఖ్యంగా నిరుపయోగమయిన కలప భిన్నాలైన, హెమిసెల్యులోజ్ మరియు లిగ్నిన్ భాగాలను బయోక్రూడ్ ఉత్పత్తికి ఉపయోగించబడాయి. ప్రస్తుత ప్రణాళికా ప్రక్రియలో హెచ్టిఎల్ ద్వారా బయోక్రూడ్ ఉత్పత్తి, డీప్ యూటెక్టిక్ ద్రావకాలను (డిఇఎస్) (deep eutectic solvents-DES) ఉపయోగించి బయోక్రూడ్ నుండి బయో-అరోమాటిక్స్ (bio-aromatics) వెలికితీత మరియు తరువాత హైడ్రోడైక్సిజనేషన్ (హెచ్డిఒ) (HDO) ద్వారా బయో-అరోమాటిక్స్ను చక్రీయ హైడ్రోకార్బన్లు (cyclic hydrocarbons) గా మార్చడం వంటి మూడు దశలు ఉంటాయి. ఈ పని యొక్క ప్రధాన లక్ష్యం హెచ్టిఎల్ పద్ధతిలో వైవిధ్య ఉత్ప్రేరకాలను ఉపయోగించి, స్థిరమైన ఉష్ణోగ్రత వద్ద మరియు సంక్లిష్ట ఇథనాల్లో తక్కువ ప్రారంభ హైడ్రోజన్ పీడనానికి ఉపయోగించడం ద్వారా బయోక్రూడ్ను ఉత్పత్తి చేయడం. ఉత్ప్రేరకాల ఎంపిక సహాయక పదార్థం యొక్క ఆమ్లత్వం మరియు మధ్యతు పై స్థిరంగా ఉండే పరివర్తన లోహం పై ఆధారపడి ఉంటుంది. ఉపయోగించిన ఉత్ప్రేరకాలు క్రింద వర్తించబడ్డాయి: బలహీనమైన మరియు మధ్యస్థమైన బ్రన్స్టెడ్ లూయిస్ ఆమ్లతత్వం (Brønsted-Lewis acidity) 5 wt. % Fe-Beta-150 లేదా ఆమ్ల రహిత 5 wt. % Fe-SiO_2. బలహీనమైన బ్రౌన్స్టెడ్ ఆమ్ల (weak-Brønsted acid) $NbOPO_4$ లేదా బలహీనంగా లూయిస్ ఆమ్లతత్వం (weak-Lewis acid)తో Pd/$NbOPO_4$.

ప్రయోగశాలలో తయారుచేసిన మరియు వర్గీకరించబడిన Fe-ఆధారిత ఉత్ప్రేరకాలు బిర్చ్ చెక్క అంశీకరణలో ఉపయోగించబడ్డాయి. వాయు వాతావరణం మరియు ఉత్ప్రేరక ఆమ్లత్వం యొక్క ప్రభావం, అలాగే ద్రవీకరణ సమయంలో ఫినోలిక్ ఉత్పత్తుల నిర్మాణం 5 wt. % Fe-H-Beta-150 లేదా 5 wt. % Fe-SiO_2 ఉత్ప్రేరకాల సమక్షంలో అధ్యయనం చేయబడింది. ప్రయోగాల తరువాత, ద్రవ, ఘన మరియు వాయు ఉత్పత్తులను అనేక విశ్లేషణాత్మక పద్ధతులను ఉపయోగించి పూర్తిగా వర్గీకరించారు. పొందిన ఫలితాలు, 5 wt. % Fe-H-Beta-150 బ్రున్స్టెడ్-లూయిస్ ఆమ్ల ఉత్ప్రేరకం, సుమారు 25 wt. % బయోక్రూడ్ ఉత్పత్తి చేయబడింది. ఆ బయోక్రూడ్ 68 wt. %. % సుగంధ ఉత్పత్తులు, ఆమ్ల రహిత 5 wt. % Fe-SiO_2 ఉత్ప్రేరకం కేవలం 18 wt. % బయోక్రూడ్ 38 wt. % తో సుగంధ ఉత్పత్తులు మాత్రమే ఇచ్చింది. బ్రున్స్టెడ్ ఆమ్ల ఉత్ప్రేరకం చెక్క కరిగే సామర్థ్యాన్ని పెంచుతుంది, ముఖ్యంగా హెమిసెల్యులోజ్ మరియు లిగ్నిన్ క్షీణత వల్ల బయోక్రూడ్లోకి ఆమ్లాలు, ఈస్టర్లు మరియు సుగంధ సమ్మేళనాలు పెరుగుతాయి. సాపేక్షంగా తక్కువ మొత్తంలో వాయు ఉత్పత్తులు ఏర్పడుతాయి మరియు ద్రవీకరణ సమయంలో ఉత్ప్రేరక కరగటం తక్కువగా ఉంటుంది. ఘన చెక్క యొక్క అవశేషాలను ఎక్స్-రే డిఫ్రాక్షన్ (XRD) కొలతల ఆధారంగా, ద్రవీకరణ సమయంలో నిరాకార సెల్యులోజ్ భాగం నుంచి స్ఫటికాకార స్థితికి మారుతుంది.

ద్రవ దశ విశ్లేషణ ఫలితాలు నిర్దిష్ట సమయంలో, 5 wt. % Fe-H-Beta-150 లేదా 5 wt. % Fe-SiO_2 ఉత్ప్రేరకాలు వాడిన సందర్భబమ్ లో లిగ్నిన్ క్షీణత ఉత్పత్తుల కోసం ఒక ప్రతిచర్య విధానం ప్రతిపాదించబడింది. ప్రధాన లిగ్నిన్ క్షీణత ఉత్పత్తి ఐసోయుజెనాల్ (isoeugenol), మరికొన్ని మధ్యంతర ఉత్పత్తులు, అనగా కోనిఫెరిల్ (coniferyl alcohol), మరియు సినాపైల్ ఆల్కహాల్ (sinapyl alcohol), 4-ప్రొపెనిల్ సిరింగోల్ (4-propenyl syringanol), సిరింగరేసినోల్ (syringaresinol), సిరంజిల్డిహైడ్రో (syringaldehyde)తోపాటు మరింత వేగంగా స్పందించాయి. ప్రతిపాదిత ప్రతిచర్య యంత్రాంగానికి మద్ధతు ఇవ్వడానికి, జాబ్యాక్ (Joback) విధానం మరియు గిబ్స్-హెల్మ్హోల్ట్జ్ (Gibbs-Helmholtz) సమీకరణాన్ని ఉపయోగించి థర్మోడైనమిక్ విశ్లేషణ కూడా జరిపాం. Nb-ఆధారిత ఉత్ప్రేరకాల విషయంలో, $Pd/NbOPO_4$ ఉత్ప్రేరకం తడి-చొరబాటు (wet-impregnation) పద్ధతి ద్వారా తయారు చేయబడింది మరియు పూర్తిగా వర్గీకరించబడింది. $Pd/NbOPO_4$ పై ప్రతిచర్య పరిస్థితులు అనుకూలపరచబడ్డాయి. ఉత్ప్రేరక ద్రవీకరణను (catalytic liquefaction) తాజా మరియు అసిటోన్ సేకరించిన బిర్చ్ చెక్క తో పోల్చారు. అదనంగా, బిర్చ్ చెక్క ద్రవీకరణపై మద్ధతు (support) మరియు లోహం (metal) యొక్క ప్రభావం నిర్ణయించబడ్డాయి. ద్రవ దశ ఫలితాల నుండి, లిగ్నిన్ క్షీణత లో ప్రధాన ఉత్పత్తి హోమోసిరింగల్డిహైడ్ (homosyringaldehyde), 5 wt. % Fe-H-Beta-150 కు ఐసోయుజెనాల్ ప్రధాన ఉత్పత్తి, విరుద్ధంగా $Pd/NbOPO_4$ కు సినాపైల్ ఆల్కహాల్ యొక్క హైడ్రోజనేషన్ను డైహైడ్రోకోనిఫెరిల్ ఆల్కహాల్ కు ఉత్ప్రేరకపరిచింది. $Pd/NbOPO_4$ పై తాజా కలప చర్య చేయబడిన, ఫలితంగా 34 wt. % ఫినోలిక్ మోనోమర్లలో 76.9 wt. % డైమెథాక్సిఫెనాల్స్ మరియు 16.5 wt. % గుయాకోల్ సంబంధిత మోనోమర్లలో ఏర్పడ్డాయి. $Pd/NbOPO_4$ ఉత్ప్రేరకంపై అసిటోన్ నుంచి సేకరించిన బిర్చ్ చెక్క ద్రవీకరణ చర్య చేయబడి 35 wt. % లిగ్నిన్ మోనోమర్ల లో 93.2 wt. % డైమెథాక్సిఫెనాల్స్ మరియు 6.8 wt. % గుయాకాల్ ఆధారిత మోనోమర్లలో కలిగిన ఫలితాన్ని ఇచ్చింది. $Pd/NbOPO_4$ పై తాజా మరియు అసిటోన్ నుంచి సేకరించిన బిర్చ్ చెక్క యొక్క ద్రవీకరణ సమయంలో డీలిగ్నిఫికేషన్ సామర్థ్యం కూడా నిర్ణయించబడింది. ద్రవ దశ ఫలితాల ఆధారంగా ఈ క్రింది ప్రతిచర్య విధానం ప్రతిపాదించబడింది: ఈథర్ బాండ్ల చీలిక ద్వారా లిగ్నిన్ క్షీణత సంభవిస్తుంది, ఇది ఘన ఆమ్ల ఉత్ప్రేరకంలో లూయిస్ యాసిడ్ సైట్ల (Lewis acid sites) చే ఉత్ప్రేరకమవుతుంది. ఆ తరువాత, తక్కువ హైడ్రోజన్ ప్రారంభ పీడనంలో Pd-మెటల్ ద్వారా మోనోఫెనాల్స్ యొక్క డీహైడ్రేషన్/ డీకైలేషన్ (dehydration/dealkylation) చర్య సంభవించింది. ఇంకా, బయోక్రూడ్ నుండి సుగంధ భాగాన్ని తీయడానికి ఒక నవల వెలికితీత పద్ధతి అభివృద్ధి చేయబడింది. కోలిన్ క్లోరైడ్ (choline chloride): ఇథిలీన్ గ్లైకాల్ (ethylene glycol) (1: 4 మోల్) తో కూడిన డీప్ యూటెక్టిక్ ద్రావకం (DES) ను మిథైల్ ఐసోబుటిల్ కెటోన్ (ఎంఐబికె) (methyl isobutyl ketone-MIBK) ద్రావకంతో మరియు నీటితో దశల వారీ పద్ధతిలో ఉపయోగించబడింది.

List of publications

I. **Jogi, R.,** Mäki-Arvela, P., Virtanen, P., and Mikkola, J-P. A Sustainable bio-jet fuel: An alternative energy source for aviation sector, *Biorefineries: A Step Towards Renewable and Clean Energy* (Verma, P, Ed.), Chapter 18, (2020) (pp. 465–496) (Springer Singapore, eBook ISBN 978-981-15-9593-6).

II. **Jogi, R.,** Mäki-Arvela, P., Virtanen, P., Mikkola, J-P. Catalytic liquefaction of wood for production of biocrude (A mini-review). *Current topics in catalysis* 14 (2019) 69–82.

III. **Jogi, R.,** Mäki-Arvela, P., Virtanen, P., Kumar, N., Hemming, J., Smeds, A., Lestander, T. A., and Mikkola, J-P. Biocrude production through hydro-liquefaction of wood biomass in supercritical ethanol using iron silica and iron beta zeolite catalysts. *Journal of Chemical Technology and Biotechnology* 94, 11 (2019): 3736–3744.

IV. **Jogi, R.,** Mäki-Arvela, P., Virtanen, P., Kumar, N., Hemming, J., Russo, V., Samikannu, A., and Mikkola, J-P. Understanding the formation of phenolic monomers during fractionation of birch wood under supercritical ethanol over iron based catalysts. *Journal of the Energy Institute* 93 (2020) 2055–2062.

V. **Jogi, R.,** Samikannu, A., Mäki-Arvela, P., Virtanen, P., Hemming, J., Mukesh, C., Lestander, T. A., Xu, C., and Mikkola, J-P. Liquefaction of lignocellulosic biomass into phenolic monomers over multifunctional Pd/$NbOPO_4$ catalyst. (Submitted).

Ramakrishna's contribution to articles I–V

I. Wrote a part of the book chapter.
II. Wrote the review article.
III. Conducted all experiments and wrote the article.
IV. Conducted all experiments and wrote the article.
V. Conducted all experiments and wrote the article.

List of other contributions

1. **Jogi, R.,** Mäki-Arvela, P., Virtanen, P., Kumar, N., Hemming, J., Smeds, A., Lestander, T. A., and Mikkola, J-P. Hydro-liquefaction of birch wood in supercritical ethanol using iron silica iron beta zeolite catalyst. 6th International Congress on Green Process Engineering (GPE), Toulouse, France, June 2018. *Poster presentation*.

2. **Jogi, R.,** Mäki-Arvela, P., Virtanen, P., Kumar, N., Hemming, J., Russo, V., Samikannu, A., and Mikkola, J-P. Kinetics for production of phenolic compounds in birch fractionation under supercritical ethanol. 14th European Congress on Catalysis (EuropaCat), Aachen, Germany, August 2019. *Oral presentation.*

Table of contents

1. Introduction (I)

In the transportation sector, aviation has a prominent part to play in the world economy, and it is an important tool to transport people and freights between different countries. The emerging aviation sector leads to the enhancement of anthropogenic CO_2 emissions, whereas in the coming 20 years the expected fuel requirements will be doubled.[1–2] Increasing demand of the fossil fuel in the transportation sector results in a continuous growth of greenhouse gas emissions (GHG). The growth of the world population and the consumption of the fossil resources causes a need to search for sustainable alternative resources to safeguard our future fuel supply. International Energy Agency (IEA) reports stated that biofuels can have the capability, in terms of alternative energy source, to fulfil the aviation fuel requirements in near future. This type of fuels can be used without any jet-engine modifications. Thus, the main significance is to upgrade a proficient and sustainable process for the production of green aviation fuel.[3–4]

1.1. Definition of bio-jet fuel (I)

A bio-jet fuel is defined as a fuel, which is produced from bio-based feedstock such as vegetable oils, waste cooking oils, sugars, animal derived fats, lignocellulosic biomass, forest residue, etc. through a sustainable biochemical or thermochemical technology. The required carbon chain length is between C_8–C_{16}, which can be used directly in an existing aviation turbine engine without any engine modifications.[5–8] Based on the feedstock and different conversion techniques, bio-jet fuels can be divided into conventional and advanced bio-jet fuels (Scheme 1).

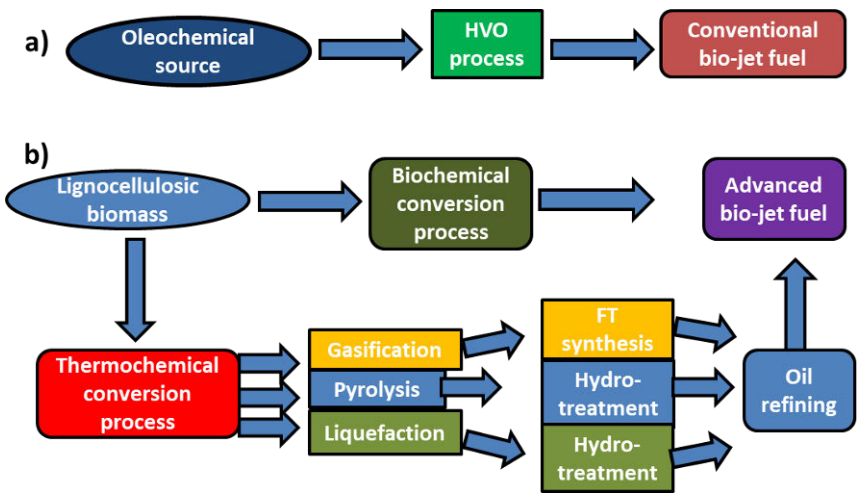

Scheme 1. Schematic representation of bio-jet fuel production paths based on different feedstock, a) conventional bio-jet fuel and b) advanced bio-jet fuel. Notations: HVO-hydro treated vegetable oils, FT- Fischer-Tropsch technology (**I**).

1.2. Conventional bio-jet fuel (I)

The conventional bio-jet fuels are produced *via* a hydrotreatment of bio-based oils (HVO) (Scheme 1a), such as non-edible vegetable oils, animal fats, waste cooking oils, etc. The oleochemical-based fuels are named as hydro-processed esters and fatty acids (HEFA) bio-jet fuels and technologies are industrially well-established. The HVO process is a combination of hydrogenation, hydrodeoxygenation, decarboxylation, isomerization and hydrocracking reactions. Oleochemical based bio-jet fuels are produced in high amounts. However, because of feedstock accessibility, sustainability and competition between bio-jet and biodiesel requirements, one cannot fulfil the demand. These needs can be fulfilled by applying this main technology to produce fuel from bio-oil derived from lignocellulose. [9-11]

1.3. Advanced bio-jet fuel (I)

The forthcoming goals to reduce the consumption of fossil fuels can only be attained by applying advanced technologies, such as biochemical[13] or thermochemical conversion [14–20] (gasification to Fischer–Tropsch synthesis, pyrolysis- Fischer–Tropsch synthesis and liquefaction) (Scheme 1b) to produce advanced bio-jet fuel. In search of viable feedstock for the production of advanced bio-jet fuel, lignocellulose based feedstock is abundant with a reasonable price and not competing with the food chain.[12]

In biochemical conversion technologies (Scheme 1b), the major obstacle is the high cost for production of middle distillates for external aviation field customers, thus there is a need to develop this type of fuel in less expensive way.[13] As an alternative, thermochemical conversion technologies to produce advanced bio-jet fuels have been developed.

In thermochemical conversion process (Scheme 1b), gasification-FT synthesis process has been previously well developed for coal gasification-FT synthesis and it doesn't need major research investment. The main desired properties of the fuels produced through gasification-FT synthesis are sulphur free, having a high thermal stability and high specific energy. Furthermore, it releases a lower amount of anthropogenic carbon. However, thermochemical process also have some drawbacks, for example low density, low aromatic content of the fuel and high capital investment needed in bio-based jet-fuel production through this technology. Due to these drawbacks, it has gained less interest when compared with other technologies.[14–20]

Bio-jet fuel can also be produced from bio-oil *via* direct liquefaction methods *e.g.* pyrolysis or hydrothermal liquefaction (HTL). In pyrolysis, the whole wood biomass is depolymerised in the absence of oxygen into bio-oil containing about 40% moisture. The further hydro-treatment of bio-oil requires high hydrogen pressure. These issues increase the production and equipment costs. There is a small advantage with pyrolysis

process; it can be performed inside a conventional oil refinery, thus reducing the capital investment on the reactor system.[21–24]

In order to develop a sustainable process to produce green aviation fuel and in comparison with other thermochemical conversion techniques; liquefaction of wood biomass has some benefits in comparison with pyrolysis.[25] In this process, two of the main wood components, hemicellulose and lignin, which currently are underutilised, can be refined into bio-jet fuel.[25]

1.4. Current status of the applied technologies to produce bio-jet fuel

Different process technologies have already been developed to produce oleochemicals derived jet fuels. For example, Neste and Honeywell UOP companies have developed process technologies to produce bio-jet/diesel fuels (hydro-processed esters and fatty acids, HEFA) from animal fats and vegetable oils.[8] The production of lignocellulosic sugar derived jet fuels have also attained more interest in Academia.[26–27] Nevertheless, these bio-jet fuels have low volumetric heat energies and low densities (about 0.76 g/ml) when compared with conventional petro-jet fuel. In order to reach these required specifications, alternative bio-jet fuels have been produced, *via* blending them with fossil derived-jet fuels.[28] Moreover, the density requirements are more demanding especially in military applications, which are used for missile propulsion. One example is JP-10 fuel, which is comprised completely of exotetrahydrodicyclopentadiene (exo-THDCPD, $\rho \approx 1.0$ g/ml).[29] The aforementioned values cannot be reached with current alternative bio-jet fuels and therefore specific fuel blends should be developed.[30]

Cyclic hydrocarbons have the ability to produce dense jet fuels with high thermal stability.[31] The production of cycloalkanes on a large scale is expensive since the feedstock is coming from hydrocracking of petroleum and has a complex composition.[32] The biomass based cycloalkanes have been produced using different alternative paths, such as alkylation of biomass intermediates for instance aromatics, furfural and cyclopentanone.[33–35]

The current work is focusing on the production of bio-oil that contains aromatics through catalytic liquefaction of lignocellulosic biomass under low initial hydrogen pressure. Bio-aromatics are the major products in bio-oil and they can be used as feedstock for the production of cyclic hydrocarbons, which exhibit an adequate density in bio-jet fuel.

1.5. Catalytic liquefaction of wood biomass (II)

Liquefaction of wood biomass is a process analogous to the fossil fuel formation under earth crust over millions of years. The conventional wood liquefaction process has been performed in water under super-critical conditions (over 373 °C and 226 bar) (**III**). The

liquefied products contain relatively low amounts of water-insoluble oil products with a high heating value compared to water-soluble products with a lower heating value and higher oxygen content, thus resulting in formation of low-heating value liquid products.[36] Due to these drawbacks, an alternative solvent with a low critical point and high miscibility with biomass needs to be identified. Polar protic solvents, for example primary alcohols such as methanol, ethanol, and propanol as well as polar hydrogen donor solvents (*e.g.* tetralin) have the ability to liquefy wood biomass, and can be used to promote gasification or liquefaction *via* solubilising wood to either in liquid or gaseous form (**II**). Different heterogeneous catalysts have been used in liquefaction of wood biomass under high hydrogen pressure to produce bio-oil such as Pd,[37] Ru,[37] Pt,[38] Ni,[39] Co,[40] CoMo,[41] and Fe,[42] supported on carbon,[37] alumina,[39] and zeolite.[37,39,42,43,44] In catalytic liquefaction of wood, the main liquid products are phenolic monomers originating from lignin. Several parameters can affect direct wood liquefaction such as reaction temperature, gas atmosphere, solvent and co-solvent effect (**II**).

The current study was focused on the performance of two transition metal modified catalysts in liquefaction of Silver birch (*Betula pendula* Roth.) to produce bio-aromatics. The selected catalysts were 5 wt. % Fe-H-Beta-150 (weak and medium Brønsted-Lewis acid sites) or 5 wt. % Fe-SiO_2 (non-acidic) (**III**) as well as $NbOPO_4$ (weak and medium Brønsted-Lewis acid sites) or Pd/$NbOPO_4$ (Lewis acid) (**V**). The catalysts were applied in catalytic liquefaction of birch to produce bio-aromatics in supercritical ethanol under low initial hydrogen pressure. After the reaction, the wood fractionation products were comprehensively characterized with GC-MS/FID, solid-state ^{13}C-MAS-NMR, SEM, acid hydrolysis, methanolysis and Klason lignin, *etc*. From the results of liquid product analysis, the reaction mechanism for formation of lignin degradation products during the fractionation was proposed. To support the proposed reaction mechanism of the Fe-based catalysts, a thermodynamic analysis was carried out by Joback approach and using Gibbs-Helmholtz equation (**IV**). In addition, a new DES based liquid-liquid extraction method was proposed to extract the aromatic fraction from bio-crude for further hydrodeoxygenation (HDO) to produce high dense cyclic hydrocarbons.[45]

2. Experimental

2.1. Materials

The used chemicals for Fe-based catalysts synthesis were ferric nitrate nonahydrate (Fluka, ≥ 98%), silica gel 60 (Merck) and, pyridine (ACROS ORGANICS, >99.5%). The used zeolites were procured from Zeolyst International (Valley Forge, PA, USA) in the ammonium form, calcined at 400 °C in order to obtain them in the proton forms.

For the synthesis of Nb-based catalyst synthesis, ammonium dihydrogen phosphate (Merck, 99%), niobium (V) chloride (Sigma-Aldrich, 99%), HCl (VWR, 37%) and palladium (II) chloride (Sigma-Aldrich, 99.9%), were used without further purification. Air, H_2 (99.99 %) and He (99.99 %) were purchased from Air Liquide Gas AB (Sweden) and used as received.

Upon the liquefaction process, ethanol (ALTIA Oyj, 99.5%), hydrogen (AGA Oy, 99.999%) and argon (AGA Oy, 99.999%) were used. Silver birch (*Betula pendula* Roth.) was received from the Swedish University of Agricultural Sciences, Umeå, Sweden, and used as a model species for a lignocellulosic feedstock.

The used chemical for the determination of leached Fe, Pd, Nb, P contents, used acids HNO_3, H_2O_2 with suprapur grade, from Merck. A commercial calibration standard Multi-Element calibration standard 3, PE#N9300233, from Perkin-Elmer used.

In the extraction process of aromatics, deep eutectic solvent (DES) was prepared using choline chloride (Sigma-Aldrich, ≥ 98.5%), ethylene glycol (Sigma-Aldrich, 99.8%), and methyl isobutyl ketone (Sigma-Aldrich, ≥ 98.5%) and they were used without further purification.

2.2. Catalyst synthesis

2.2.1. Iron (Fe)-based catalysts (**III**)

5 wt. % Fe-H-Beta-150 catalyst was synthesized using the evaporation impregnation method (EIM), in which ferric nitrate nonahydrate was dissolved in 250 ml of water and pH was measured (**III**). Beta zeolite was added to ferric nitrate solution and the mixture was stirred for 24 h at 60 °C. After that, water was evaporated. The catalyst was dried at 100 °C overnight and calcined in a muffle furnace for 4 h at 450 °C (**III**).

5 wt. % Fe-SiO_2 catalyst was synthesized using ultra sound-evaporation impregnation (US-EIM) method (**III**). The silica particles were added to ferric nitrate solution to form a slurry, which was first exposed to ultrasound for 2 h, and kept on rotation for 24 h. The aqueous solution was finally evaporated and the catalyst was dried for 7 h at 100 °C and calcined in a muffle oven at 250 °C for 50 min and thereafter

heated with the rate of 3.3 °C /min to 450 °C, and held at this temperature for 3 h, and cooled to 25 °C (**III**).

2.2.2. Niobium (Nb) based catalysts (**V**)

The support $NbOPO_4$ was prepared under hydrothermal conditions using niobium penta chloride ($NbCl_5$) as the niobium (Nb) precursor and ammonium dihydrogen phosphate ($NH_4H_2PO_4$) as the phosphate precursor, respectively. In a typical preparation, the required amount of niobium chloride precursor was dissolved using conc. HCl solution (37%) at 80 °C. Thereafter, a small extra stoichiometric quantity of ammonium dihydrogen phosphate (with respect to the concentration of Nb) was dissolved separately in conc. HCl solution (37%), and added to the above mixture and stirred for 5 h at 80 °C. The final material was filtered, washed thoroughly with deionized water, dried overnight at 100 °C and finally calcined at 450 °C for 5 h.[46]

The Pd containing $Pd/NbOPO_4$ catalyst was prepared by applying a wet-impregnation method using palladium (II) chloride ($PdCl_2$) as the Pd precursor. The nominal loading of Pd was fixed to 5 wt. %. In a classic synthesis, the support ($NbOPO_4$) was dispersed in a required amount of deionized water. Then, a calculated amount of palladium chloride precursor solution (dispersed in deionized water) was slowly added to the above slurry under stirring. The obtained mixture was stirred for 5 h. Thereafter, the solvent was evaporated from the slurry and the catalyst was dried overnight at 100 °C. At the end, the catalyst was calcined at 400 °C for 3 h (temperature was raised 2 °C/min under airflow of 30 ml/min). Finally, the catalyst was reduced prior use at 400 °C for 3 h under 10 ml/min of H_2 flow (temperature was risen 2 °C/min) and stored in 10 ml ethanol until used.[46–47]

2.3. Catalyst characterization

2.3.1. Nitrogen physisorption (**III, V**)

The textural properties of prepared Fe-based catalysts, such as specific surface area and pore volume were measured with Sorptomatic 1900 instrument and calculated with B. E. T. as well as Dubinin's methods, respectively.[26] For Nb-based catalysts adsorption-desorption isotherms were determined with Micrometrics ASAP 2010 apparatus, specific surface area was calculated using B. E. T. method and Barrett, Joyner and Halenda (BJH) algorithm was used to determine the pore size.[47] (**III, V**).

2.3.2. Pyridine FT-IR

The acidity of the Fe and Nb-based catalysts were measured by pyridine adsorption-desorption with an ATI Mattson FT-IR instrument (**III, V).**[48] The quantity of Brønsted and Lewis acid concentrations at 1545 cm^{-1} and 1455 cm^{-1}, respectively, were calculated using the molar extinction factors from Emeis.[48]

2.3.3. X-Ray powder diffraction (XRD)

Niobium based catalysts were characterized with PANalytical diffractometer using Cu Kα (λ=0.154 nm) radiation to measure the small (2θ range of 0.5–10°) and wide (2θ range of 10–70°) angle powder X-ray diffraction patterns of the catalyst with the count of 15 sec at each point in the steps of 0.025° (**V**).[46]

2.3.4. Field-emission scanning electron microscopy (FE-SEM)

The surface morphology and elemental composition of the Nb-based catalysts were characterized using a field-emission scanning electron microscopy (FESEM, Carl Zeiss Merlin GmbH) equipped with energy-dispersive X-ray spectroscopy (EDS, Oxford Instruments X-MAX 80 mm^2) at 5 kV (**V**).[46]

2.3.5. Transmission Electron Microscopy (TEM)

The surface morphology of the $Pd/NbOPO_4$catalyst was determined with transmission electron microscopy (TEM) JEOL 1230, it works at 80 kV (**V**).[46]

2.3.6. Inductively Coupled Plasma Mass Spectrometry (ICP-MS) and Inductively Coupled Plasma Optical Emission Spectrometry (ICP-OES) (**III, V**)

Iron content leached into reaction medium was determined by ICP-MS. In the preparation of sample, 3 ml of sample was first pipetted into a Teflon vessel, and evaporated at 80–130 °C. Then 5 ml of nitric acid (HNO_3) (60%) and 1 ml of hydrogen peroxide (H_2O_2) (30%) were added. Thereafter, the sample was dissolved in a microwave oven (Anton Paar Multiwave-3000, Graz, Austria), sample diluted to 100 mL and, further diluted 1/5 prior to ICP-MS (Perkin-Elmer, Waltham, MA, USA, Elan 6100 DRC Plus) analysis. Iron was analyzed in DRC mode, with ammonia as the reaction gas (**III**).

In Nb-based catalysts, the leached metal content in liquid phase was determined by ICP-OES with Optima 4300 DV optical atomic emission spectrometer. The retrieval stay time was set to 90 s and 1000 scans, respectively, were collected.[50] The preparation of sample for the determination of leached metals was as follows: The liquid sample (5 ml) was taken and ethanol was evaporated under N_2 flow at 40 °C. The sample was dissolved in 1.5 vol. % of HCl prior to analyzing its palladium (Pd) content. In the same way, 5 ml of the sample was evaporated and dissolved in 1.5 vol. % of HNO_3 for the determination of its niobium (Nb) and phosphorous (P) content, respectively.[50]

2.4. Hydrothermal liquefaction of wood (III, IV, V)

The wood liquefaction process was performed in supercritical ethanol (243 °C) over Fe- or Nb- based catalysts using 5 bar hydrogen initial pressure at room temperature. The applied reactor system is depicted in Fig. 1. In a typical experiment for Fe-based catalysts, 7.6 g of fresh birch wood with the particle size $<$ 0.1 mm, 10 wt. % moisture was soaked in

100 ml ethanol.[36] In case of Nb-based catalysts, 4 g dry-weight with particle size ≤ 250 µm, and 30 wt. % moisture of the fresh birch was soaked in 90 ml ethanol overnight. Freshly reduced $Pd/NbOPO_4$ stored in 10 ml ethanol was added to the reaction mixture (**V**). Meanwhile the required amount of $NbOPO_4$ support (previously dried at 100 °C overnight) was directly added to 100 ml ethanol containing birch that was soaked overnight (**V**). The hydrothermal liquefaction experiments were performed in an autoclave (Parr stirred reactor, 300 ml capacity, 4560 mini bench top reactor). Initially, the reactor system was flushed with N_2 and then with H_2 for five times to remove the residual air. Thereafter, the reactor was filled with 5 bar H_2 at room temperature (**III**) and heated with 10°C/min heating rate and stirred approximately 50–100 rpm during heating. During this time the reaction medium reached 243 °C and this was taken as the starting point for the reaction. The reaction starting point was taken at the point when the reaction medium reached 243 °C (**III**). The liquid samples were collected at different time intervals during the experiment. After a certain time, the reactor was cooled down to room temperature by applying a cold-water cooling coil inside the reactor. When the room temperature was reached, gas samples were collected for GC-TCD/FID (Gas Chromatography coupled to Thermal Conducting and Flame Ionization Detectors) analysis (**III)**. In the final stage, liquid and spent wood samples were separated with Whatman filter paper (Grade-50, diameter-70 mm, and circles-100) for further characterization (**III**).

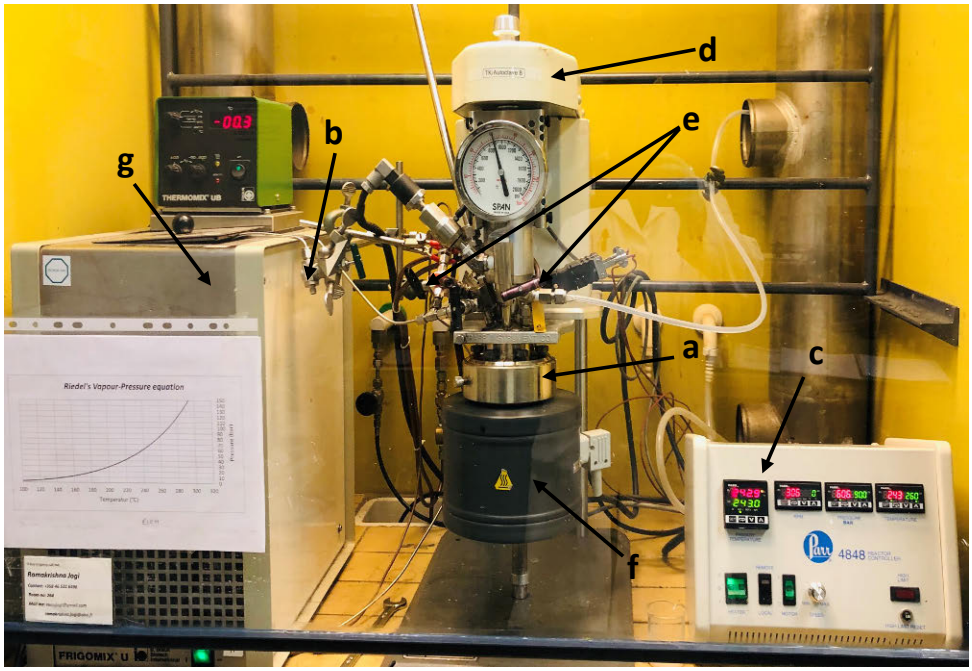

Fig 1. A photograph of the use reactor system. Notations: **a**) reactor chamber, **b**) liquid sampling valve, **c**) control and measurement unit, **d**) stirrer, **e**) gas inlet and outlet, **f**) heating jacket, and **g**) cooling unit.

2.5. Analysis of products and feedstock (III)

The fresh and spent biomasses was analyzed by various methods in order to obtain a complete picture of the feedstock and the different products, containing liquid and solid phases (Scheme 2) (**III**). In addition, the morphological studies of the fresh and spent wood were performed by p-XRD, SEM and Solid-state ^{13}C-MAS-NMR (**III**).

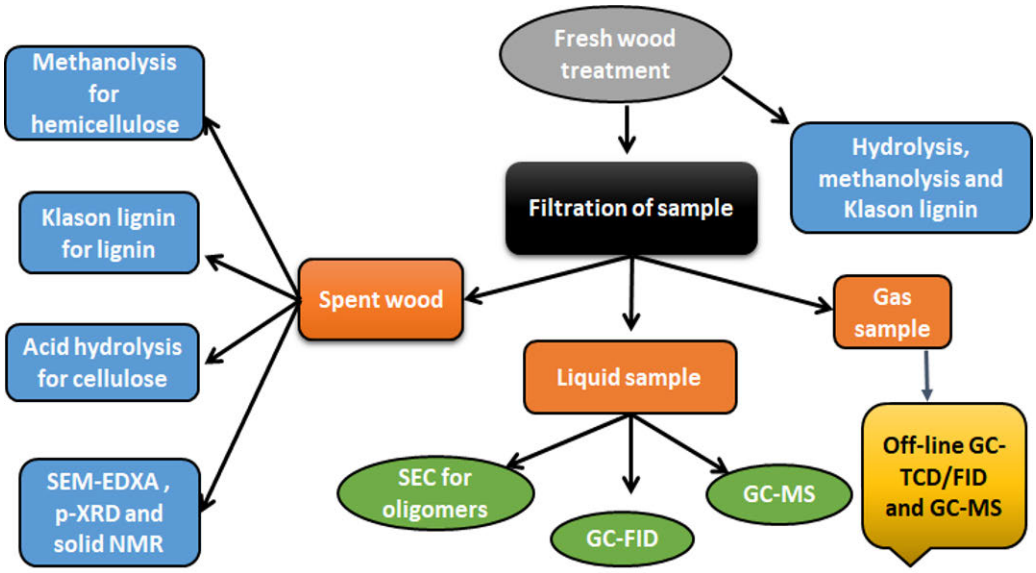

Scheme 2. Schematic representation of product and wood biomass analysis. Notations, SEM-EDXA: Scanning Electron Microscope/Energy Dispersive using X-Ray (Analysis), p-XRD: X-ray Powder Diffraction, solid NMR: Solid state ^{13}C magic angle spinning (MAS) nuclear magnetic resonance (NMR), SEC: Size-Exclusion Chromatography, GC-MS: Gas Chromatography–Mass Spectrometry, GC-FID: Gas Chromatography-Flame Ionization Detector (**III**).

2.5.1. Solid phase analysis (**III, V**)

In this study, fresh and acetone extracted birch were used as a feedstock. The feedstock and products were characterized according to Scheme 2 (**III**, **V**).

Lipophilic extractives such as fatty and resin acids were separated from freeze dried birch using Accelerated Solvent Extractor (ASE-200, DIONEX) in acetone-water medium (95: 5 vol. %) at 100 °C with 35 bar pressure for 5 min static time in 3 cycles (**V**).[49]

2.5.1.1. Determination of cellulose content (acid hydrolysis) (**III, V**)

10 mg of the freeze-dried wood sample and with the calibration sample (10 mg cotton linters), were transformed into two test tubes. One glass ball was added into each test tube and thereafter 0.2 ml of sulfuric acid (72%) was added in each tube. The sample was depressurized in vacuum oven and after kept in fume hood for 2 h. Then 0.5 ml of

distilled water was added in each test tube and let to rest for another 4 h, after which 6 ml of distilled water was added in each test tube and the samples were kept overnight in the fume hood. The next day, the test tubes were put in an autoclave at 125 °C for 90 min and cooled to room temperature. Thereafter 1-2 drops of bromocresol reagent was added and mixed well. After that, a small amount of $BaCO_3$ was added until color changed occurred (yellow to blue). Then 1 ml of internal standard (5 mg/ml sorbitol) was added to the samples and centrifuged. From that, 0.5 ml of the top layer was taken, into a few ml of pure acetone was added and the sample was dried over N_2 flow in water bath at 40 °C. The obtained samples were silylated in pyridine (150 µl) with HMDS (150 µl) and TMCS (70 µl), kept in a fume hood for overnight and analyzed with GC (**III, V**).

2.5.1.2. Determination of hemicellulose content (methanolysis) (**III, V**)

Calibration samples were first prepared by adding 1 ml of a carbohydrate calibration solution, which is 0.1 mg/ml in methanol. Samples were evaporated under nitrogen flow at 50 °C.

For the fresh and spent wood samples, 10 mg of feeze-dried wood was weighted in a pear-shaped flask. 2 ml of methanolysis reagent (2M HCl in methanol) was added to each wood sample and evaporated calibration samples. The samples were kept in an ultrasonic water bath for about 1 min. Thereafter, samples were shaken well and put in an oven kept at 100 °C for 5 h. After that, the samples were allowed to cool down to room temperature to equalize the pressure. 1 ml of internal standards (0.1 mg/ml sorbitol + resocrcinol + pentaerythritol in methanol) were added to the calibration samples and 4 ml of the same internal standard was added to the real samples as well, and mixed well. 1.5 ml of samples from each pear-shaped flask was transformed to another test tube and further dried under nitrogen flow at 40 °C. The obtained samples were depressurized in vacuum oven for 20 min to remove the residual solvents. Thereafter, the samples were silylated with 150 µl of pyridine, 150 µl of HMDS and 70 µl of TMCS and mixed well with a vortex mixture. Then further analyzed by GC in below mentioned conditions.

*2.5.1.3. Determination of lignin content (Klason lignin) (**III, V**)*

15 ml of 72 % H_2SO_4 was drop wise added to 1 g of freez dried wood sample and mixed well with a glass rod. After that, the sample was left to settle at room temperature for 2 h, with the glass rod left in the beaker during that time. After that, 575 ml of distilled water was added to the sample. The sample was boiled for 3 h and water was added during that time to maintain the liquid amount unaltered. After that the sample was let to cool down and the lignin was allowed to sediment overnight. Thereafter, the samples were filtered through glass fiber filter paper. The collected filter paper was dried in oven at 100 °C and weighed. The obtained result was reported as Klason lignin insoluble

(mg/g). The filtrates were used to determine the Klason soluble lignin content through UV spectrophotometer at 205 nm (**III, V**).

2.5.1.4. X-Ray Powder Diffraction (p-XRD) (**III, V**)

The morphological changes of the fresh and the spent birch from Fe-based catalyst experiments were measured by p-XRD (Bruker AXS D8 Discover, Karlsruhe, Germany) with a Cu K-α X-ray source. The crystallinity index (CI) was defined as the amount of crystalline material in total cellulose of the fresh and the spent biomass by p-XRD and calculated according to Scherrer's approximation method (**III**). The ratio of the height of the peak area (I_{002}) at 2Θ=22.5° and minimum peak height at 2Θ=18° peak area (I_{AM}) referred as CI using the following equation:

$$L = 0.9(\beta \cos \Theta) - 1 \quad (1)$$

Where λ = 1.542 Å, β is the full width at the half of the maximum (FWHM) defined from fitted peak curves and Θ is the diffraction angle (2Θ=22.2°) (**III**).

The morphological changes of the fresh and the spent birch sample from Nb-based catalyst experiments were determined by PANalytical diffractometer with Cu Kα (λ=0.154 nm) radiation with the small (2θ range of 0.5–10°) and wide (2θ range of 10-70°) angle powder X-ray diffraction patterns of the wood with the span of 15 sec at each point in the steps of 0.025°.[46]

2.5.1.5. Solid-state ^{13}C-MAS-NMR (**III**)

In Fe-based catalyst experiments, the fresh and the spent birch samples were characterized by Solid-state ^{13}C-MAS-NMR (Bruker 600MHz).

2.5.1.6. Field Emission-Scanning Electron Microscopy (FE-SEM) (**V**)

SEM images were taken from the fresh and spent birch wood using the field-emission scanning electron microscopy (FE-SEM, Carl Zeiss Merlin GmbH) equipped with an energy-dispersive X-ray spectroscope (EDS, Oxford Instruments X-MAX 80 mm^2) at 5 kV.

2.5.2. Liquid phase analysis (**III, V**)

From all the collected liquid samples, 0.2 ml sample was dried in a water bath at 40 °C under N_2 flow and kept in vacuum oven for about 10 min to remove the residual gases. Thereafter, the sample was silylated with 150 µl using the mixture of pyridine, N,O-bis (trimethylsilyl) trifluoroacetamide (BSTFA), and trimethylchlorosilane (TMCS) reagents in the ratio of 1: 4: 1, then placed in an oven at 70 °C for 45 min and analyzed quantitatively with GC-FID and the reaction products were identified with GC-MS (**III, V**).

2.5.2.1. GC-FID analysis (**III, V**)

The silylated samples were quantitatively analysed by GC-FID (Clarus 500, Perkin Elmer, Inc., Waltham, MA, USA); two columns: 25 m, 0.20 mm i.d., 0.11 mm HP-1 and HP-5 columns in parallel and a 6–7 m, 0.530 mm i.d., 0.15 mm HP-1/SIMDIS column (Agilent Technologies, Inc., Santa Clara, CA, USA) (**III, V**).

Qualitative identification of compounds was done by GC-MS. GC-MS analyses were performed with an HP 6890-5973 GC-quadrupole-MSD instrument (Hewlett-Packard, Palo Alto, CA, USA) equipped with 25-m HP-1 GC column, 25 m, 0.20 mm i.d., and 0.11 µm film thickness. The identification was based on a comparison to compounds found in the spectral libraries of mass spectra.

2.5.2.2. Size Exclusion Chromatography (HP-SEC-ELSD) (**III, V**)

For the preparation of a sample for SEC analysis, 5 ml of liquid sample was evaporated in the presence of N_2 at 50 °C in hot water bath to remove the residual solvents and ethanol. After that, the obtained sample was prepared as 1 mg/mL concentration with tetrahydrofuran (THF). These liquid samples were analysed using a high-performance (HP) SEC-evaporative light scattering detector (ELSD) (**III, V**).

In HP-SEC-ELSD (Shimadzu Corporation, Japan), the columns were two 300 mt, 7.8 mm *i.e.* Jordi Gel DVB 500A (Columnex LLC, New York, NY, USA) columns in series, and a 7.5 m* 4.6 mm guard columns. The column oven was kept at 408°C, the eluent THF/alcohol 99:1 (v/v) exhibited the flow rate was 0.8 ml min^{-1}, the analysis time was 28 min, and the HPLC nebulizer was kept at 40 °C at an air pressure of 3.5 bar (**III, V**).

2.5.3. Gas phase analysis (**III**)

0.5 ml of the collected gas phase samples were analyzed by GC-TCD/FID as followed conditions. A gas chromatograph (Agilent 6890N GC with TC and FI detector) utilized a column HP-PLOT Q with a length of 60 m, inner diameter 0.53 mm and film thickness of 33 µm. The temperature was first held at 35 °C for 8 min, then raised 20 °C/min to 230 °C and, held for 30 min and raised to 350 °C for 8 min.

2.6. Aromatic fraction extraction with deep eutectic solvent (DES) (V)

2.6.1. DES preparation (**V**)

The DES preparation was done as follows: the pre-dried choline chloride (ChCl) and ethylene glycol (EtGly) were dried under vacuum overnight, a mixture of ChCl: EtGly with the molar ratio of 1:4 was prepared in a beaker under magnetic stirring with 1400 rpm for one hour at 60 °C until a colorless liquid was formed.[42] The obtained liquid was stored in a closed bottle for further extraction purpose.[51]

2.6.2. Extraction of aromatic fraction (**V**)

The objective of this study was to develop an extraction process to extract aromatic fraction from bio-crude produced through direct liquefaction or pyrolysis of biomass. All the liquid-liquid extractions were performed in a 100 ml separation funnel at 25 °C. The extraction process contains the following steps (Fig 2): In the first step, the bio-crude was mixed with an optimized amount of distilled water (30 ml) to separate the water-soluble sugars, esters, acids and aromatic fraction in the non-polar bio-oil. Aqueous phase and bio-oil mixture was shaken well with water (**A**) and allowed to stabilize overnight to reach equilibrium. Thereafter the separation of aqueous phase (**2a**) from non-polar bio-crude fraction (**1a**) was done. Among that, the aqueous phase (**2a**), 30 ml of non-polar solvent and methyl isobutyl ketone (MIBK) were used to extract the phenolic fraction (**F, G**). The extraction of the aromatic fraction with the 30 ml of MIBK from the aqueous phase takes place in a single extraction.

Afterwards, the remaining non-polar bio-crude phase (**1b**) was solubilized in 30 ml of DES (ChCl: EtGly) (**B**) and mixed well to make a homogeneous phase. This non-polar phase also contained aromatic compounds along with sugars, fatty acids, esters. Then, a non-polar solvent (30 ml) (**1c**) was added to the homogeneous mixture; even though, an extensive phenolic extraction could not be attained by the addition of the non-polar solvent (**1c**). This result was most possibly due to existence of strong hydrogen bonds between phenolic compounds and DES. To overcome this challenge, 30 ml distilled water was added into DES: bio-crude mixture and non-polar solvent (**1d**). Water acts as an anti-solvent for DES (it can break DES into its building blocks) and as a result, the aromatic fraction was transferred from DES: water phase (**6**) to the non-polar phase (**5**). An aromatic fraction extraction with a non-polar solvent from DES: water phase (**C, D, E**) can be achieved in 2-3 steps with 30 ml of the fresh non-polar solvent. The same non-polar solvent was applied in the aqueous phase extraction (**2b**) to extract the non-polar biocrude phase (**1b**).

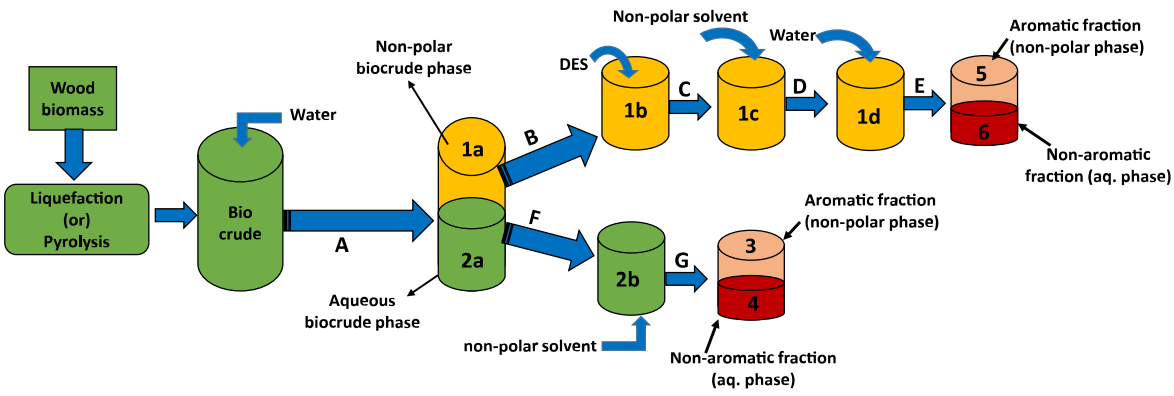

Fig 2. A schematic representation of aromatic fraction extraction from biocrude using deep eutectic solvent (DES) **(V)**.

3. Results and discussion (III, IV, V)

3.1. Fe-based catalysts (III, IV)

Two Fe-based catalysts with different acidities, 5 wt. % Fe-H-Beta-150 and 5 wt. % Fe-SiO_2 were tested in wood liquefaction in supercritical ethanol. In addition, the influence of the gaseous atmosphere was evaluated. The Fe-based catalysts characterization results can be seen in Table 1. The acidities of the Fe-based catalysts were confirmed by using Pyridine FT-IR.

Table 1. Characterization results of catalysts (**III**)

Catalyst	Specific surface area (m^2/ g_{cat})	Pore volume (cm^3/g_{cat})	Acid sites (µmol/g_{cat})		
			250°C	350°C	450°C
3.1% wt. Fe-Beta-150 (EIM)	587	0.209	192 [a] 165 [b]	162 [a] 45 [b]	14 [a] 2 [b]
4.6% wt. Fe-SiO_2 (US-EIM)	389	0.68	4 [a] 5 [b]	4 [a] 3 [b]	2 [a] 1 [b]

[a] Brønsted acid sites, [b] Lewis acid sites (**I**).

3.1.1. Influence of gas atmosphere (**III**)

The depolymerisation of wood biomass was performed in supercritical ethanol, under either argon or hydrogen atmosphere and the results are shown in Table 2. The degradation of wood biomass was higher in hydrogen than under an inert atmosphere, *e.g.* 26 wt. % of wood dissolution was obtained under hydrogen while only 19 wt. % efficiency was obtained under inert atmosphere.

From the GC-MS analysis of the liquid phase, in total 420 components were identified and among those only 64 components were quantified by GC-FID. These components were divided into 3 main groups, such as acid-esters, sugars, and phenolics. The depolymerisation degree of wood was increased in the absence of catalyst under hydrogen atmosphere when compared to argon. In the presence of hydrogen, the formation of sugars and phenolic components increased. For example, 3.3 fold more isoeugenol was formed under hydrogen than under argon atmosphere. Analogous trend was observed for the formation of syringaresinol and sinapyl alcohol under hydrogen atmosphere.

The remaining solid residues were analyzed by using methanolysis, acid hydrolysis, and Klason lignin methods to acquire the amount of main wood components, cellulose, hemicellulose and lignin content. The cellulose-to-hemicellulose ratio with the fresh birch was 1.4, while it was in the spent wood under argon 2.2 and when treated under hydrogen 1.9 (Table 2). These results showed that even though supercritical ethanol treatment enhances the dissolution of birch in the absence of a catalyst, only minor dissolution of hemicellulose was obtained. Similarly, the weight ratio between cellulose to lignin increased from the fresh birch to hydrogen or argon treated solid residue, even though the gas atmosphere had a minor influence on lignin elimination. The dissolution rate of birch was increased in hydrogen. Hemicellulose and lignin dissolutions occurred with the same rates independently on the gas atmosphere.

Table. 2. The results from the dissolution of birch **(III)**

Entry	Name of the sample	Total dissolution of biomass[a] (wt. %)	Bio-oil yield[a] (%)	Cellulose content[a], [b] (wt. %)	Hemicellulose content[a], [b] (wt. %)	Lignin content[a], [b] (wt. %)	Cellulose to hemi-cellulose weight ratio[a], [b]	Cellulose to lignin weight ratio[a], [b]
1	Fresh birch	-	-	44	31	25	1.4	1.8
2	No catalyst (Ar)	19	13	55	25	24	2.2	2.3
3	No catalyst (H_2)	26	19	50	26	23	1.9	2.2
4 (a)	5 wt. % Fe-H-Beta-150 (H_2)	33	25	56	20	12	2.8	4.7
4 (b)	5 wt. % Fe-H-Beta-150 (H_2)	31	24	52	21	10	2.5	5.2
5	5 wt. % Fe-SiO_2 (H_2)	20	17	53	24	23	2.2	2.3

[a] Birch wood- relative content of dry solid, [b] Analysis of solid residue, *Entry 4(a) and 4(b) runs for reproduce bility of results.

3.1.2. Influence of catalyst acidity (**III**)

3.1.2.1. Overall birch dissolution efficiency (**III**)

Out of the two evaluated Fe-based catalysts, 5 wt. % Fe-H-Beta-150 was more efficient whereupon the overall dissolution efficiency of birch was 33 wt. % under hydrogen in supercritical ethanol (Table 2). The experimental error from the reproducibility tests with this catalyst was only 6%, which is tolerable. In case of the non-acidic 5 wt. % Fe-SiO_2, the dissolution efficiency of birch was 20 wt. %, which is very close to the level obtained in the absence of catalyst under argon atmosphere (Table 2). The results showed that the biomass was efficiently dissolved in the presence of an acidic catalyst, while Fe-SiO_2 catalyst was not efficient in birch dissolution. The highest bio-oil yield from birch was 25 wt. % over 5 wt. % Fe-H-Beta-150 catalyst, while in case of 5 wt. % Fe-SiO_2, it was only 17 wt. %. Water has an acidic nature under current reaction conditions.[52] The presence of moisture in the wood together with a high temperature enables an efficient wood dissolution over a Brønsted-Lewis acidic catalyst. The high dissolution efficiency of wood over 5 wt. % Fe-H-Beta-150 catalyst comparison to that over 5 wt. % Fe-SiO_2 in birch dissolution can be qualitatively seen in SEM pictures of the solid residue indicating that the wood morphology was more ruptured than in case of the fresh wood (Fig 3).

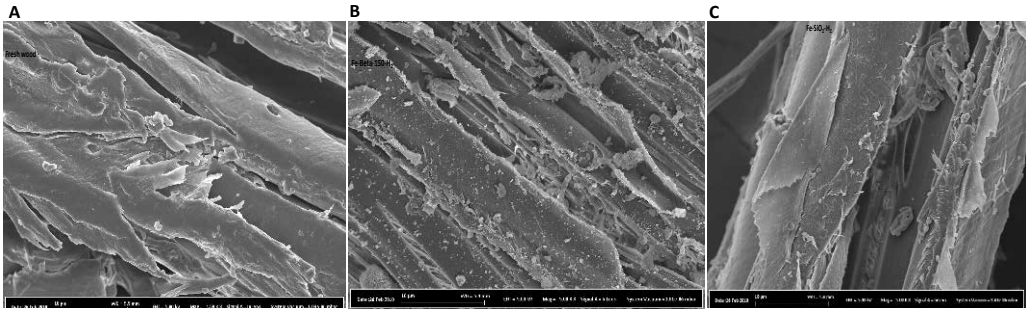

Fig 3. SEM pictures of the fresh and the spent biomass: (A) fresh birch; (B) 5 wt. % Fe-H-Beta-150 (hydrogen); (C) 5 wt. % Fe-SiO_2 (hydrogen) (**III**).

Current results of wood dissolution are in good agreement with the results by Xu *et al*.[53] where the dissolution degree of pine was 30 % in the absence of catalyst at 225 °C under 50 bar of initial hydrogen pressure in 40 min reaction time. In the current work with birch as feedstock, 26 wt. % dissolution was obtained. Nevertheless, it should be kept in mind that the initial hydrogen pressure in the present work was only 5 bar, although the total pressure at reaction conditions (243 °C) was 63 bar. In the results from the Xu *et al.*[44] the pine conversion 88 wt. % was reported over a homogeneous catalyst, 5 wt. % $FeSO_4$ under 50 bar H_2 pressure at 350 °C. In the present work birch conversion was 33 wt. % and it was attained under 63 bar total pressure at 263 °C over

5 wt. % Fe-H-Beta-150 catalyst. The homogeneous catalyst is clearly more efficient than the heterogeneous one, however, it is more difficult to separate from the formed bio-oil and re-use in following batches.

3.1.2.2. Liquid phase analysis (**III**)

The obtained liquid phase products were determined by GC-MS and quantified by GC-FID, and the results indicated that 5 wt. % Fe-H-Beta-150 catalyst treated wood samples contained significant quantities of acids-esters, phenolics, and sugars. Remarkably, isoeugenol was present in the liquid products. Earlier it was reported by Huang *et al*.,[53] that the main products obtained under 30 bar hydrogen over Pd/C catalyst at 180 °C for 2 h, were alkylmethoxyphenols. The current study showed that the efficient hydrogenation of liquid products over iron catalyst had not effectively taken place. During depolymerisation of wood biomass over 5 wt. % Fe-H-Beta-150 catalyst improved the decarboxylation and esterification of acids was also improved, while the quantity of monomeric and dimeric sugars formation was reduced over strong Brønsted acid catalyst. Furthermore, the sugar molecules were not stable in presence of an acid catalyst under harsh conditions. The concentration of phenolic components was high in case of 5 wt. % Fe-H-Beta-150 catalyst. Meanwhile, in the case of 5 wt. % Fe-SiO_2 treated sample, the amount of sugar components was increased. Likewise, a significant amount of lignin depolymerisation products can be obtained both over 5 wt. % Fe-H-Beta-150 and 5 wt. % Fe-SiO_2 catalysts.

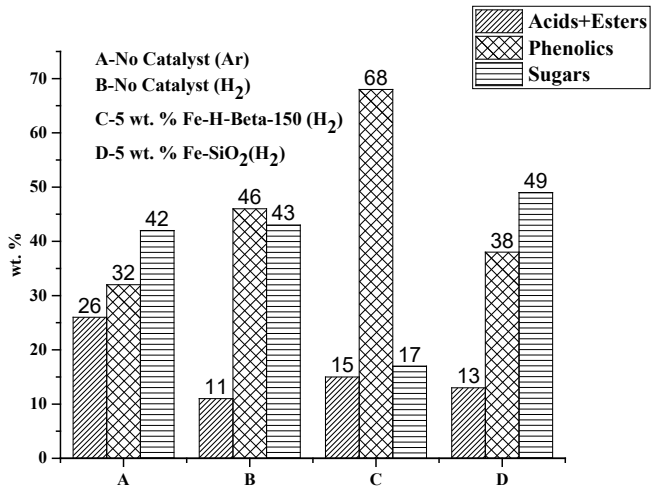

Fig 4. Relative amounts of liquid phase components after HTL treatment of wood (**III**).

In order to determine the molecular size and level of depolymerisation, the liquid phase products were analyzed by SEC. It was reported by Anderson *et al.,*[54] that during depolymerisation of corn stover lignin oligomers, *i.e.* dimers, trimer and tetramer

compounds were formed over Ni/C with 0.1 M H_3PO_4 as a co-catalyst under 30 bar hydrogen. These results were compared with those obtained in the current work over 5 wt. % Fe-H-Beta-150. The major liquid phase products exhibited above 300 g/mol molecular weight after 1 h fractionation, for instance phenolic dimers were formed. The results of SEC analysis of the liquid samples showed that the major part of products, changing the area from 75% to 87% in SEC chromatograms (Table 3), exhibited molecular weights above 300 g/mol. These compounds were determined by comparing their retention times with the standard compounds retention times (**III**). The sum of the normalized areas of compounds with the molecular mass above 300 g/mol as follows: hydrogen (no catalyst) < argon (no catalyst) < 5 wt. % Fe-H-Beta-150 < 5 wt. % Fe-SiO_2 showing that hydrogen enhanced the formation of monomers and protects them from repolymerisation, which occurred under argon atmosphere. Both Brønsted and Lewis acidity enhanced the formation of oligomers even in the presence of hydrogen. It can be concluded that Fe-based catalysts are efficient to produce phenolic compounds with high molecular weight in hydrothermal wood liquefaction.

Table 3. SEC area of liquid products above 300 g/mol molecular weight (**III**).

Name of the sample (birch)	**SEC (% area)**	**Total area normalisation**
No catalyst (Ar)	87	1.2
No catalyst (H_2)	88	1.0
5 wt. % Fe-H-Beta-150 (H_2)	89	1.3
5 wt. % Fe-SiO_2 (H_2)	75	1.4

3.1.2.3. Physical texture of the residual solids (**III**)

The residual solid phase samples were characterized by using p-XRD, ^{13}C-NMR and SEM to back the results obtained from chemical analyses. The increased crystallinity index (CI) of the residual wood samples determined by XRD (Table 4), indicated that the amorphous cellulose was more easily hydrolyzed than the crystalline one. The XRD diffractograms of cellulose I peaks gave peaks at 15.5 °, 17.0 ° and 22.2 ° of 2Θ. The CI of the treated birch over 5 wt. % Fe-H-Beta-150 (hydrogen) was higher than for 5 wt. % Fe-SiO_2 (hydrogen) treated birch (Fig. 5). These results can be explained by the presence of Brønsted-Lewis acid sites in 5 wt. % Fe-H-Beta-150, facilitating particularly dissolution of lignin from birch.

Table 4. Crystallinity index (CI) and crystal size of the fresh and residual birch wood (**III**)

Name of the sample	**Crystallinity Index (%)**	**Crystal(002) size (nm)**
Fresh birch	81	3.3
No catalyst (Ar)	88	4.1
No catalyst (H_2)	85	3.7
5 wt. % Fe-H-Beta-150 (H_2)	89	4.3
5 wt. % Fe-SiO_2 (H_2)	86	4.0

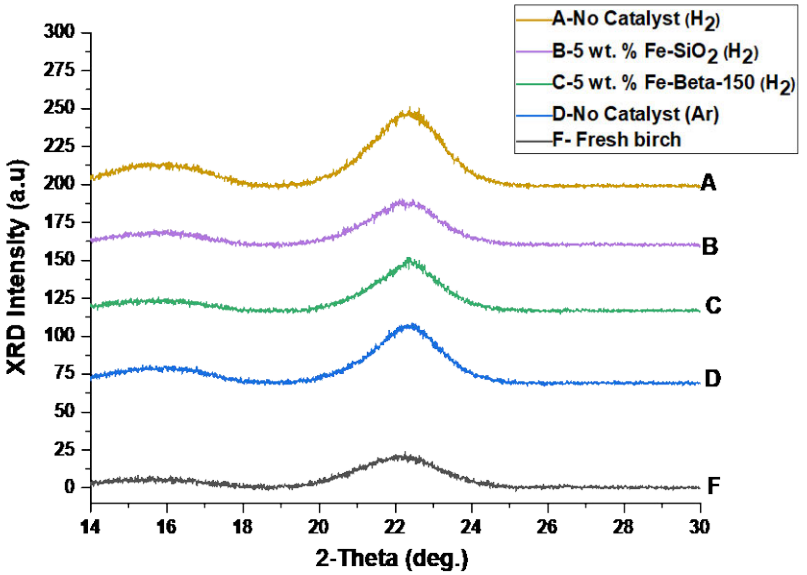

Fig 5. XRD-pattern for birch, fresh and spent wood (**III**)

The fresh and spent wood samples were analysed by ^{13}C-MAS-NMR and the results indicated that the amount of amorphous phase C-4 at the chemical shift of 84 ppm had considerably decreased in case of 5 wt. % Fe-H-Beta-150 catalyst treated birch (Fig. 6). Furthermore, the signals of lignin clearly identified at 135 and 152 ppm in fresh birch significantly decreased. In addition, the signal of methoxy group at 57 ppm had considerably decreased for the samples treated under argon and hydrogen over 5 wt. % Fe-H-Beta-150 and 5 wt. % Fe-SiO_2 catalysts.[55]

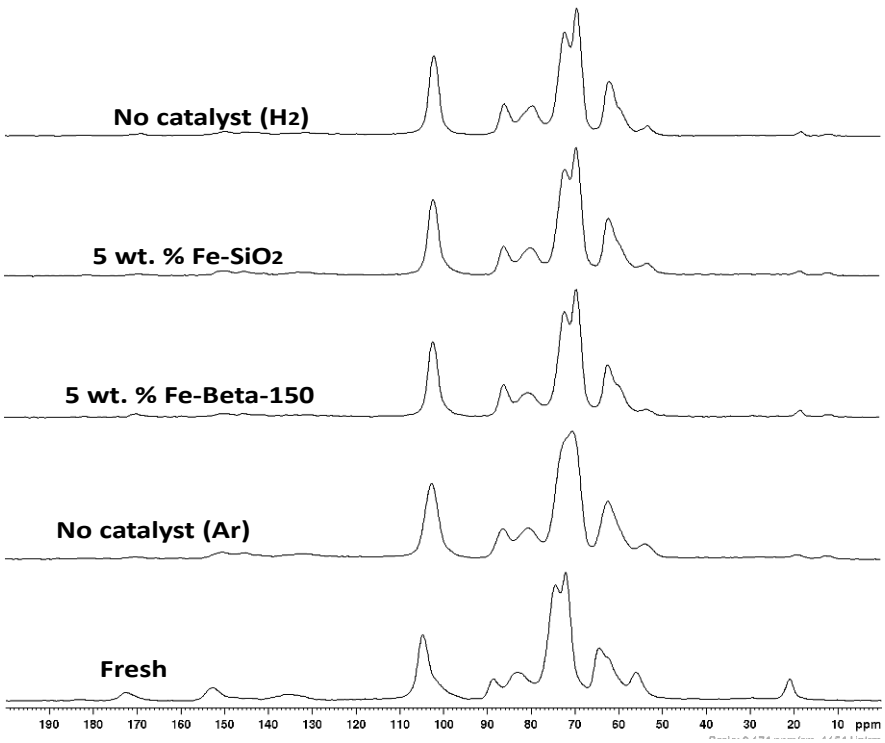

Fig 6. ^{13}C MAS- NMR from fresh and residual birch wood samples (**III**).

3.1.2.4. Analysis of gas phase (**III**)

The main product, in the gas phase under hydrogen atmosphere without catalyst, is CO_2 and only very small quantities of hydrocarbons were identified such as methane, ethane, propane, and iso-butane. Similar results were attained from the treated birch over Fe-SiO_2 catalyst. When the treatment of birch was performed over 5 wt. % Fe-H-Beta-150 catalyst, a relatively low amount of gases were detected.

3.1.2.5. Catalyst leaching (**III**)

The catalyst that performed best in the liquefaction experiments, 5 wt. % Fe-H-Beta-150, was chosen for leaching studies. As a comparison, leaching was also studied in the absence of catalyst. The obtained results indicated that the leached iron content in the liquid phase after reaction over 5 wt. % Fe-H-Beta-150 catalyst was 0.341 ppm. It is very insignificant amount, and when taking into account the harsh reaction conditions, some leaching is predictable. Biomass moisture content enhances the acidity of the reaction medium. Furthermore, ethanol has a high pKa value at supercritical point, which increases leaching of the catalyst.

3.2. Formation of phenolic products from the fresh birch during in liquefaction (IV)

The phenolic monomer formation during wood fractionation was studied over 5 wt. % Fe-H-Beta-150 or 5 wt. % Fe-SiO_2 catalysts, even though internal and external mass transfer limitations must be present. The concentration differences in formed phenolic compounds were observed in large scale, indicating the importance of a catalyst.

The sum of phenolic monomers determined by GC-FID, indicated that the obtained amount of monomeric compounds were 2 fold over 5 wt. % Fe-H-Beta-150 compared to a non-acidic 5 wt. % Fe-SiO_2 catalyst, hence showing the superiority of the 5 wt. % Fe-H-Beta-150 catalyst. The following products were identified and quantified from liquid phase: isoeugenol, sinapyl alcohol, syringaresinol, 4-propenyl syringol, syringol, syringyldehyde, syringol acetone and coniferyl alcohol. The reaction mechanism for formation of these phenolic compounds through liquefaction of birch in supercritical ethanol was proposed (Fig. 7).

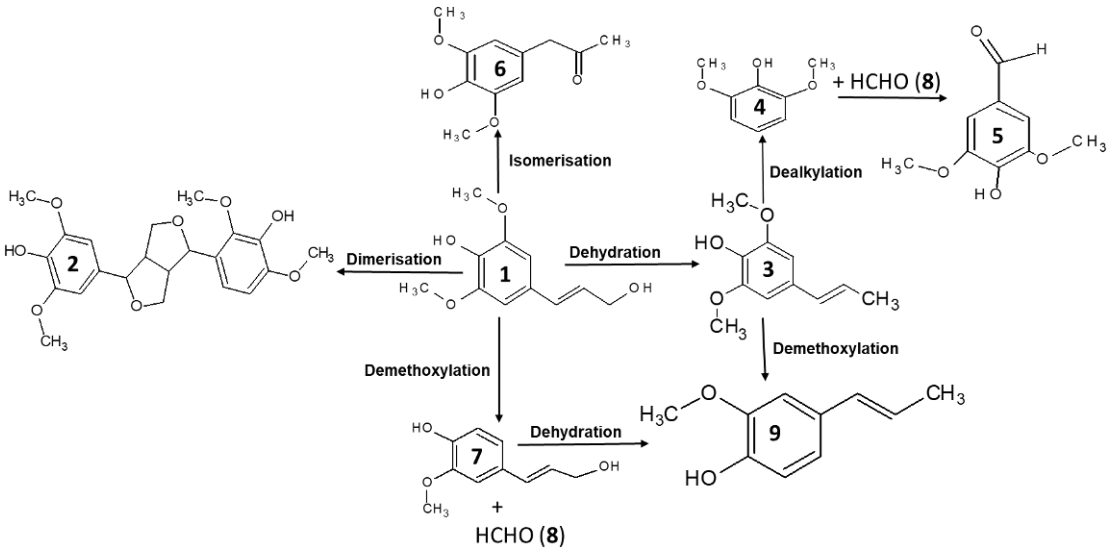

Fig 7. The proposed reaction network for the formation of phenolic compounds during birch fractionation under supercritical ethanol over 5 wt. % Fe-H-Beta-150 or 5 wt. % Fe-SiO_2. Notations: **1**. sinapyl alcohol, **2**. syringaresinol, **3**. 4-propenyl syringol, **4**. syringol, **5**. syringayldehyde, **6**. syringol acetone, **7**. coniferyl alcohol, **8**. formaldehyde and **9**. isoeugenol (**IV**).

Based on the reaction scheme (Fig. 7), syringaresinol **2** is formed by dimerization of sinapyl alcohol **1** and is stable under applied reaction conditions. Sinapyl alcohol **1** can also react to: syringol acetone **6** *via* isomerization, 4-propenyl syringol **3** *via* dehydration, coniferyl alcohol **7** *via* demethoxylation.

Sinapyl alcohol **1** undergoes isomerization in the presence of water and forms a small amount of syringylactone **6**. When 5 wt. % Fe-H-Beta-150 catalyst was applied, more syringylacetone **6** was formed, indicating that the acid catalyst enhances this reaction. Based on this a result, a reaction mechanism was proposed, which is similar to keto-enol tautomerism, the chemical equilibrium occurs among ketone-sinapyl alcohol.[57] However, it must confirmed that a small amount of sinapyl alcohol **1** is converted also into syringylacetone **6** when the distance C-C double bond and alcohol group is large. The proposed reaction mechanism to form syringylacetone **6** from sinapyl alcohol **1** is shown in Fig. 8.

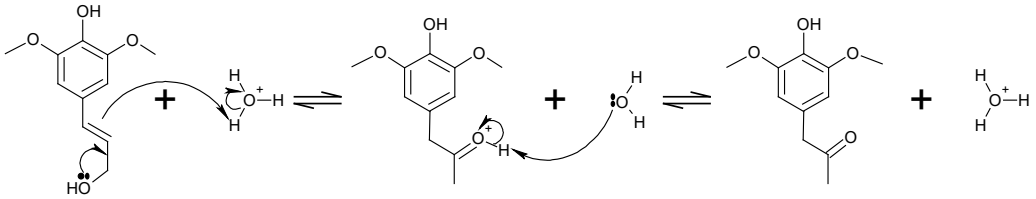

Fig 8. The proposed reaction mechanism for isomerization of sinapyl alcohol to syringylacetone (**IV**).

The formation of syringol **4** occurs through dealkylation of 4-propenyl syringol **3**. According to literature, the required bond energy for breaking of aromatic C-O bond is 456 kJ/mol, while the aliphatic C-O bond has lower bond energy 339 kJ/mol.[58-59] This enables the dehydration of sinapyl alcohol **1** to 4-proprenyl syringol **3.** Demethoxylation of an aromatic OCH_3 requires bond dissociation energy of 376 kJ/mol.[58] However, the cleavage of an aromatic OCH_3 is much easier than the cleavage of an aromatic C-O bond. The influence of Brønsted and Lewis acid sites is not only to break bonds between lignin ether and carbohydrate ester, but also break the β-O-4 bonds in lignin exclusively.[60-61] Thereafter, the conversion of propanolsyringol into propanol and ethylsyringol through hydrogenation and decarbonylation reactions occurs.[64] In reactive lignin model compounds experiments, acidity of catalyst has an important role. Ether bond cleavage occurs as a result of dehydration reaction after protonation of the hydroxyl group located on the leading carbon, which stabilize carbocation. Particularly the presence of Brønsted-Lewis acid sites is important for dehydration.[63-65] From the experimental results, it has been confirmed that the presence of electron donating groups promotes ether bond breaking, for example methoxy/hydroxyl substituents enhance ether bond cleavage in lignin.[64-65]

Demethoxylation of sinapyl alcohol **1** to coniferyl alcohol **7** and formaldehyde **8**, and further hydrogenation to methanol was inefficient over Fe catalyst. In the next step, the formed formaldehyde **8** can be combined to syringol **4** resulting in the formation of syringylaldehyde **5**. Similarly, to sinapyl alcohol **1** with 4-propenyl alcohol **3** in the side

chain, coniferyl alcohol **7** can easily undergo dehydration forming isoeugenol **9.** These results are supported with the data in the literature,[39] where the formation of lignin monomer in the fractionation of extracted birch over Ni/Al_2O_3 catalyst at 250 °C in methanol under 30 bar initial hydrogen was studied. However, the reported main product was propanol syringol and propanol guaiacol showing the high hydrogenation ability of Ni/Al_2O_3 catalyst.[39] In the current work, the main product was isoeugenol **9**, followed by syringaldehyde **5**, and syringaresinol **2** obtained in the presence of the most acidic catalyst, 5 wt. % Fe-H-Beta-150. Acid sites are enhancing the formation rates of alkylated products such as reaction between syringol **4** with formaldehyde **8** (Fig. 7) and combination of two sinapyl alcohol **1** molecules occurring through dehydration (Fig. 7). As a function of time, the concentration of sinapyl and coniferyl alcohol decreased as expected. Isoeugenol rapidly hydrogenated particularly in the presence of Pt- or Ni- supported catalysts,[66-67] however, this reaction did not proceed over 5 wt. % Fe-H-Beta-150 showing that iron possesses a low hydrogenation ability.

The ratios between the initial rates for parallel routes were also calculated for the different compounds in wood fractionation based on molar weights (Fig. 9) (Table 5). From those results, it can be observed that an acidic catalyst 5 wt. % Fe-H-Beta-150 catalyst promotes the formation of isoeugenol **9** through dehydration and demethoxylation reactions.

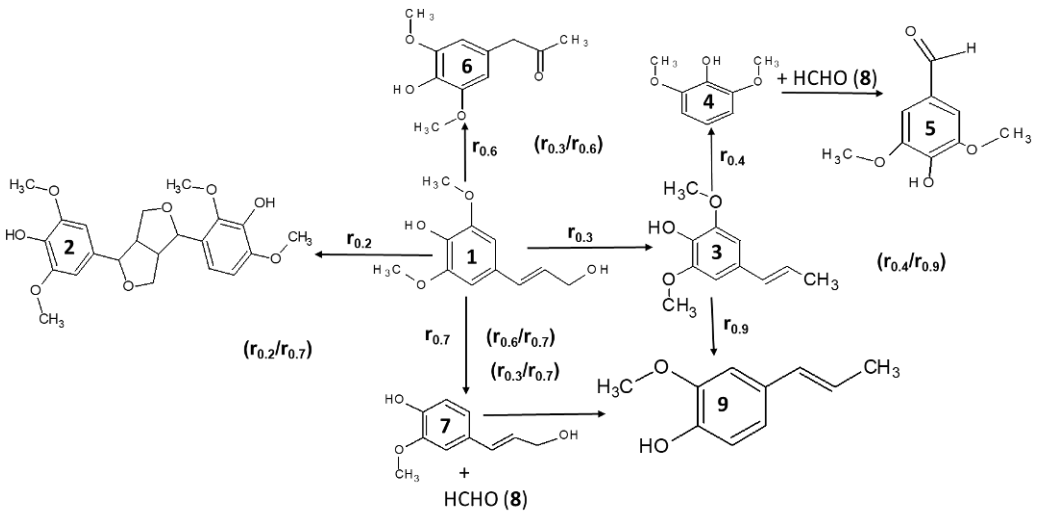

Fig 9. The proposed reaction network for birch fractionation over 5 wt. % Fe-H-Beta-150 or 5 wt. % $Fe-SiO_2$, the initial reaction rates for formation of phenolic compounds in birch fractionation under supercritical ethanol are compared. Notation: **1**. sinapyl alcohol, **2**. syringaresinol, **3**. 4-propenyl syringol, **4**. syringol, **5**. syringyldehyde, **6**. syringol acetone, **7**. coniferyl alcohol, **8**. Formaldehyde and **9**. isoeugenol (**IV**).

Table 5. The ratio between the initial rates for formation of different phenolic products from fresh birch wood (**IV**).

Entry no	Catalyst	Addition vs. Demethoxy-lation ($r_{0.2}/r_{0.7}$)	Dehydration vs. demethoxy-lation ($r_{0.3}/r_{0.7}$)	Dehydration vs. isomerizati-on ($r_{0.3}/r_{0.6}$)	Isomerizatio n vs. Demethoxyl-ation ($r_{0.6}/r_{0.7}$)	Dealkylation vs. Demethoxyl-ation ($r_{0.4}/r_{0.9}$)
1	5 wt.% Fe-H-Beta-150 (Fresh birch, 1 h run time)	5.25	8.45	2.30	3.8	0.07
2	5 wt. % Fe-SiO_2 (Fresh birch, 1 h run time)	0.42	0.48	3.10	0.50	0.25
3	No catalyst (Fresh birch, 1 h run time)	0.22	0.28	3.80	0.18	0.70

3.3. Enthalpy and Gibbs free energy changes for fractionation of phenolic compounds (IV)

Enthalpy (ΔH^0_r) and Gibbs free energy (ΔG^0_r) were calculated at standard conditions by following a thermodynamic method,[68] whereas the calculations were done by using CHEMCAD v.7.0 software, starting from the standard Enthalpy (ΔH^0_f) and Gibbs free energy (ΔG^0_f) of formation from the elements estimated with Joback approach,[69-71] *Eqs.* 2–3.

$$\Delta H^0_{r,j} = \sum_j \nu_{i,j} \cdot \Delta H^0_{f,i} \quad (2)$$

$$\Delta G^0_{r,j} = \sum_j \nu_{i,j} \cdot \Delta G^0_{f,i} \quad (3)$$

The equilibrium constant of each reaction was calculated from its definition,

$$K_j^0 = \exp\left(-\frac{\Delta G_{r,i}^0}{RT}\right) \quad (4)$$

The dependency of the Gibbs free energy with temperature was included by implementing the Gibbs-Helmholtz equation valid at P=1 bar ($\Delta G^{\Phi}_{r,j}$) as follows,

$$\frac{\Delta G_{r,j}^{\phi}(T)}{T} = \frac{\Delta G_{r,j}^0}{T^0} + \Delta H_{r,j}^0\left(\frac{1}{T} - \frac{1}{T^0}\right) \quad (5)$$

The stoichiometric matrix was built based on the reaction scheme reported in Table 6. The calculated Enthalpy and Gibbs free energy for formation of each component (i) are reported in Table 7 at standard reaction conditions.

Table 6. Enthalpy and Gibbs free energy for formation of each component (*i*) and stoichiometric matrix for component *i* for reaction *j* (**IV**).

Component	**ΔH^0_f [J/mol]**	**ΔG^0_f [J/mol]**	***i/j***	**1**	**2**	**3**	**4**	**5**	**6**	**7**
sinapyl alcohol	$-5.34\cdot10^5$	$-2.86\cdot10^5$	**1**	-2	-1	-1	-1	0	0	0
syringaresinol	$-1.13\cdot10^6$	$-4.99\cdot10^5$	**2**	1	0	0	0	0	0	0
4-propenyl syringol	$-3.81\cdot10^5$	$-1.50\cdot10^5$	**3**	0	1	0	0	-1	-1	0
syringol	$-4.25\cdot10^5$	$-2.45\cdot10^5$	**4**	0	0	0	0	0	1	-1
syringyl aldehyde	$-5.43\cdot10^5$	$-3.46\cdot10^5$	**5**	0	0	0	0	0	0	1
syringyl acetone	$-6.11\cdot10^5$	$-3.59\cdot10^5$	**6**	0	0	1	0	0	0	0
coniferyl alcohol	$-3.69\cdot10^5$	$-1.80\cdot10^5$	**7**	0	0	0	0	0	0	0
formaldehyde	$-1.09\cdot10^5$	$-8.96\cdot10^4$	**8**	0	0	0	0	0	0	-1
isoeugenol	$-2.17\cdot10^5$	$-4.33\cdot10^4$	**9**	0	0	0	1	1	0	0
water	$-2.42\cdot10^5$	$-2.28\cdot10^5$	**10**	0	1	0	1	0	0	0
propane	$-1.04\cdot10^5$	$-2.44\cdot10^4$	**11**	0	0	0	0	0	1	0
hydrogen	0.00	0.00	**12**	-1	-1	0	-2	-1	-2	1
methanol	$-2.05\cdot10^5$	$-1.79\cdot10^5$	**13**	-1	-1	0	1	1	0	0

Table 7. Enthalpy and Gibbs free energy for each reaction (*j*) at standard conditions (243 °C, 63 bar), equilibrium constants at standard conditions (K^0_j) (**IV**).

J	$\Delta H^0_{r,j}$ [J/mol]	$\Delta G^0_{r,j}$ [J/mol]	K^0_j
1	-5.81E+04	7.37E+04	1.22E-13
2	-8.96E+04	-9.12E+04	9.42E+15
3	-7.76E+04	-7.23E+04	4.68E+12
4	7.47E+04	1.50E+04	2.33E-03
5	1.64E+05	1.06E+05	2.47E-19
6	-1.48E+05	-1.20E+05	1.19E+21
7	-9.09E+03	-1.11E+04	8.91E+01

Starting from these values, the Enthalpy and Gibbs free energy for each reaction (*j*) were calculated at different temperatures. A temperature range from 298.15 K–543.15 K was investigated. The results are shown in Fig. 10.

As disclosed, reactions 1 (formation of syringaresinol) (Fig. 10A) and 5 (demethoxylation of 4-propenyl **3** to isoeugenol **9**) (Fig. 10B) do not occur spontaneously in the investigated temperature range. Formation of isoeugenol was, however, possible from sinapyl alcohol with two hydrogen molecules above at T >375 K. At the same time, water and methanol were also formed ((**IV**), Fig. 10A). From the thermodynamical point of view, sinapyl alcohol is rapidly dehydrated and further transformed to isoeugenol, while the transformation of 4-propenylsyringol to isoeugenol is thermodynamically not feasible under these reaction conditions. In addition, 4-propenyl syringol **3** transformation to syringol **6** has a very low Gibbs free energy, while alkylation of syringol **4** with formaldehyde has only slightly negative Gibbs free energy (Fig. 9B).

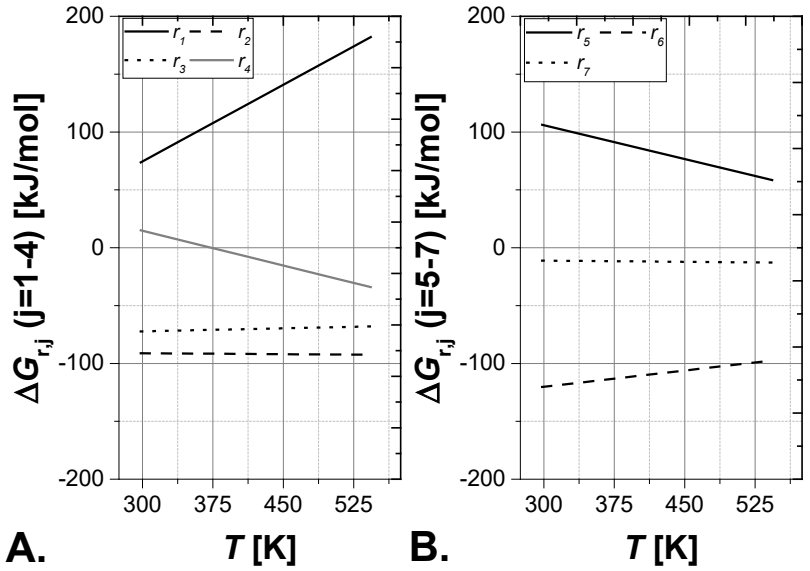

Fig 10. Gibbs free energy for each reaction (j) as a function of temperature (**IV**)

3.4. Nb-based catalysts (V)

3.4.1. The textural properties of catalysts (**V**)

In order to determine the morphological and structural properties of $NbOPO_4$ and $Pd/NbOPO_4$ catalysts, N_2 adsorption-desorption was measured by the B.E.T. method. The adsorption-desorption isotherms of $NbOPO_4$ and $Pd/NbOPO_4$ (Fig. 11a) showed a type 3 isotherm with a hysteresis loop between P/P_0 ranging between 0.4 to 1.0. B.E.T. isotherms of supported and unsupported catalysts do not show an N_2 adsorption-desorption plateau at high P/P_0, for example in case of $Pd/NbOPO_4$. Agreeing to IUPAC system, the hysteresis loop H3 indicates the occurrence of the wedge-shaped pores on the niobium support. The B.E.T. specific surface area, mean pore volume, pore diameter and Pd particle size of $NbOPO_4$ and $Pd/NbOPO_4$ are shown in Table 8. After the deposition of palladium nanoparticles on the $NbOPO_4$ support through wet impregnation method, the B.E.T surface area of the catalytic material decreased from 56 to 37 m^2/g. Remarkably, a small enlargement of the mean pore volume (0.16 to 0.17 cm^3/g) and considerable growth of mean pore diameter (11.69 to 18.21 nm) were noticed. This change can be assigned to the accumulation of the niobium support particles at some point in catalyst preparation; it might be altered in the existing porous structure. The deposition of Pd nanoparticles on the microporous pores of the carrier support, in that way the mean pore diameter is shifting towards a higher value. Furthermore, the additional pore-like structure can be formed between two Pd clusters, which can affect the mean pore size and diameter.

Table 8. Results from catalyst characterizations **(V)**

Sample	BET ($m^2\ g^{-1}$)	pore volume (cm^3/g)	pore diameter (nm)	average metal particle size (nm)	Amount of acid sites (µmol/g_{cat})		
					150°C	250°C	350 °C
NbP	56	0.16	11.69	--	65[a] 9[b]	46[a] 3[b]	25[a] 0.0[b]
5 wt. % Pd-NbP (3.58 wt. %)	37	0.17	18.21	2	12[a] 97[b]	1[a] 23[b]	0.0[a] 2[b]

$NbOPO_4$ was in crystalline form, which was confirmed by X-ray diffraction patterns with, small and wide-angle (Fig. 11b). $NbOPO_4$ exhibited peaks at 2θ, 19.7° (110), 25.6° (101), 27.8° (200), 39.7° (220), 44.8° (310), and 48.0° (301) and these peaks were also visible in $Pd/NbOPO_4$ with somewhat reduced intensity. The small intensity of the Pd diffraction was assigned to the insignificant amount of Pd nanoparticles accumulated over the niobium support. The superimposition of the echo planes from Pd metal with the crystalline niobium support directed to the nonexistence of the resultant diffraction peaks at 2θ=40 °. Moreover, the deposition of Pd on $NbOPO_4$ support, resulted in a small decrease in the support crystallinity.

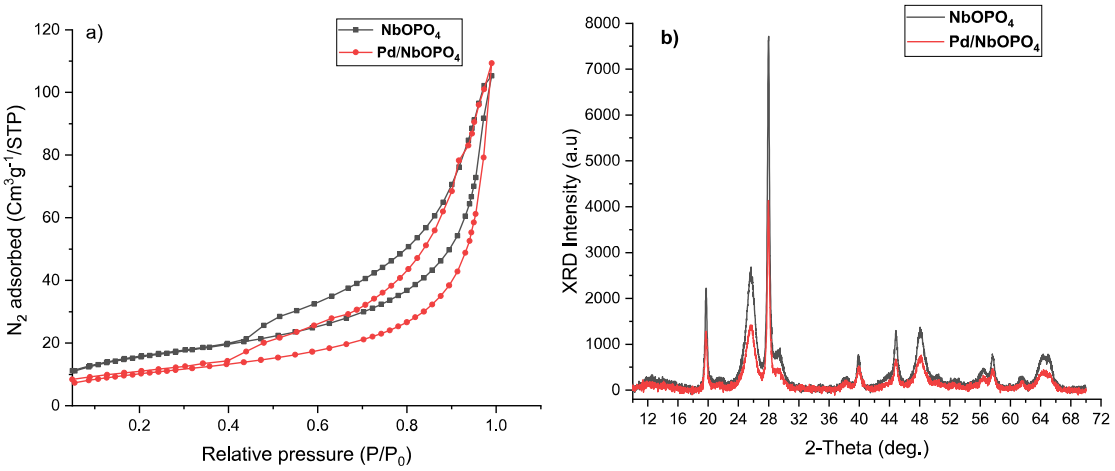

Fig 11. a) N_2 adsorption-desorption isotherms of $NbOPO_4$ and $Pd/NbOPO_4$ b) XRD pattern of $NbOPO_4$ support and $Pd/NbOPO_4$ (**V**)

The TEM images confirmed the existence of Pd nanoparticles (ca. 2 nm) over $NbOPO_4$ support. These Pd particles are too small to be visible in the XRD patterns. The lack of considerable Pd clusters and identical Pd particle (approx. 2nm) displays effective metal support interactions between Pd and niobium support, thus affecting the electrostatic interaction concerning the inter particle Pd clusters which materializes them organized. The TEM images showed that Pd particles were homogeneously loaded on the $NbOPO_4$ support. It can also be seen from TEM images that the niobium support displays the existence of wedge type pores in which Pd nanoparticles were accumulated. This microscopic image of the niobium support can be related to the wedge type pores, which were shown in the B.E.T isotherm. The catalyst surface morphology and particle distribution of Nb and P were also examined by Scanning Electron Microscopy, SEM (**V**) and EDS microelement mapping (SEM-EDS) analysis (Fig. 12). The SEM image of the $Pd/NbOPO_4$ reveled an improved surface disorderness compared to the pure niobium support. It can support the case in accumulation of niobium support in catalyst preparation, which followed in reduced crystallinity of the finishing $Pd/NbOPO_4$ catalyst. In $NbOPO_4$, peculiarly the ratio of Nb/P was close to one. EDS microelement mapping images of $NbOPO_4$ and $Pd/NbOPO_4$ indicated that the Pd particles were homogenously dispersed on the $NbOPO_4$ support. The Pd loading was slightly lower than expected from nominal loading of 5 wt. % (3.58 wt. % confirmed by SEM-EDS). Nevertheless, the abnormality was well within the experimental errors. It can be concluded that the immobilized Pd nanoparticles were uniformly dispersed over the $NbOPO_4$ support. $NbOPO_4$ exhibited a higher Brønsted acidity than Lewis acidity, though, when Pd was doped on $NbOPO_4$, some Brønsted acid sites were blocked by Pd and, consequently, the number of Lewis acid sites of the catalyst was higher than the amount of Brønsted acid sites.

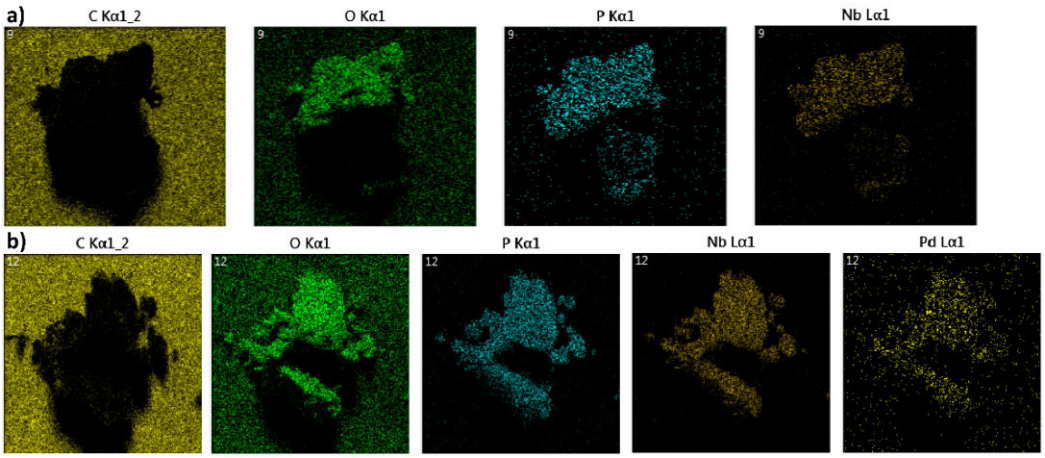

Fig 12. SEM-EDS microelement mapping (C, O, P, Nb, and Pd) of a) $NbOPO_4$ and b) $Pd/NbOPO_4$ (**V**).

3.5. Catalytic liquefaction of birch over Nb-based catalysts (V)

3.5.1. Optimization of reaction conditions (**V**)

In order to optimize the reaction conditions, the liquefaction of birch was performed over Pd/$NbOPO_4$, such as catalyst mass and stirring speed were varied, whereas the solvent volume, reaction time, initial hydrogen and temperature were kept constant.

To examine whether the birch liquefaction was performed in the kinetic regime; four different catalyst masses were applied under fixed reaction conditions (at 243 °C, 300 rpm, and 3 h). The total wood dissolution efficiency, yield of lignin monomers, and aromatic compounds in wood dissolution were determined (Table 9, in Figs. 13a, 13b). The delignification efficiency and total wood dissolution were determined by hydrolysis, methanolysis and Klason lignin methods after 3 h. According to these analysis results, the total wood dissolution and delignification efficiency were improved with increasing catalyst amount from Fig. 13a. It can be seen that 250 mg of catalyst was already feasible, whereas 700 mg was most ineffective. In contrast, when applying a high amount of catalyst the amount of lignin monomers decreased. This can occur due to strong adsorption of phenolic compounds on the catalyst surface.

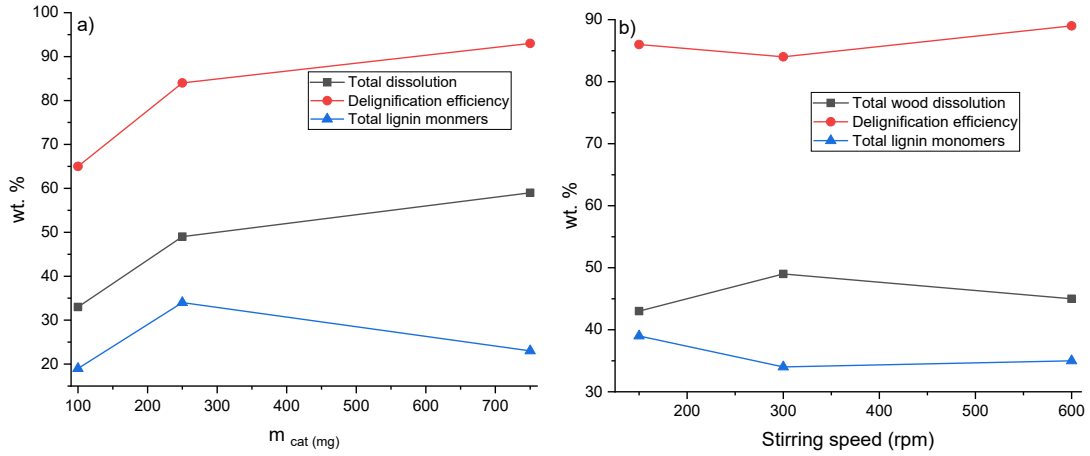

Fig. 13. Optimization of a) catalyst mass, b) stirring speed in birch dissolution over Pd/$NbOPO_4$. The values are given after 3 h reaction time (**V**).

Three different stirring speeds were applied to study the influence of external mass transfer (Fig. 13b). The results revealed that the total wood dissolution after 3 h improved from 100 rpm to 300 rpm, whereas with 600 rpm it was nearly the same as acquired with 300 rpm. It was concluded that the stirring speed of 300 rpm was acceptable to perform the experiments in the absence of external mass transfer limitations. However, stirring speed did not affect the delignification efficiency.

When applying a low amount of catalyst (100 mg), low dissolution efficiency of wood (33 wt. %) was obtained. Simultaneously, the efficiency of delignification was 65 wt. % and 19 wt. % of lignin monomers were obtained (Table 9). The initial rate for formation of aromatic compounds, defined as moles formed between 15 min and 30 min is shown as a function of catalyst mass in Fig. 14. These results revealed that r_0 was 2.3 fold higher when the catalyst mass was increased from 100 mg to 250 mg, while only 3.1 fold improvement was attained in r_0 when increasing catalyst mass from 100 mg to 750 mg. Hence, catalyst weight of 250 mg was chosen for further studies.

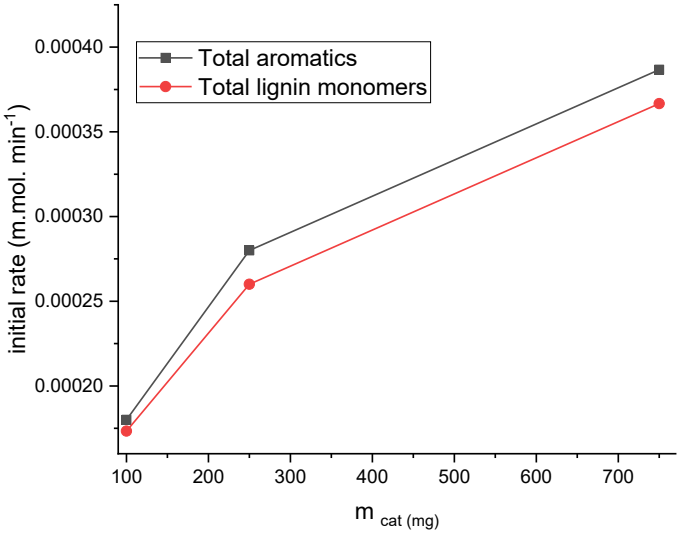

Fig 14. Initial reaction rates (r_0) for formation of aromatics and lignin derived monomers with different catalyst masses measured from GC results.

The formation of phenolic components during birch fractionation with respect to the amount of catalyst mass was studied (**V**). Under optimal reaction conditions, dimethoxyphenols were formed via effective β-O-4 bonds cleavage in lignin finally forming homosyringaldehyde (**7**) (syringol unit) as the major product and dihydroconiferyl alcohol (**9**) (guaiacyl unit) as the second major product. In addition, 4-propenyl syringol (**5**) was the third major product (Fig. 15) (Scheme 3). 4-propenyl syringol (**5**) was mainly formed when a low amount of catalyst, 100 mg was applied and the breakage of the β-O-4 bond was inefficient. In case of 250 mg of catalyst, a higher bond cleavage capacity was detected resulting in an extensive formation of homosyringaldehyde (**7**). In contrast, an increased amount of catalyst (750 mg) can considerably obstruct the formation of those compounds. The current results are analogous with the result of Van den Bosch, *et al.*[37] showing that too high catalyst amount is not beneficial and it might enhance product adsorption on the catalyst surface, which ultimately halts the reaction.

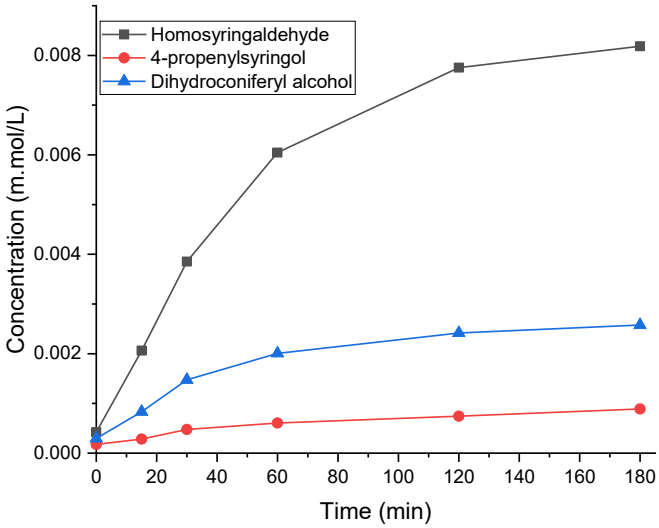

Fig 15. Concentration of the main liquid products from birch dissolution over Pd/$NbOPO_4$ as a function of time.

From the mechanistic point of view, it can be confirmed that the two main products, 4-propenylsyringol and coniferyl alcohol were formed from sinapyl alcohol as follows (Scheme 3). The cleavage of sinapyl alcohol (**1**) from lignin occurred by the cleavage of ether bonds (β-O). Further, sinapyl alcohol (**1**) was transformed via dehydration to 4-propenylsyringol (**5**), which reacted further *via* cracking/dealkylation to 4-methyl syringol (**6**). On the other hand, demethoxylation of sinapyl alcohol (**1**) resulted in the formation of coniferyl alcohol (**3**), and formaldehyde (**4**). Owing to the incapability of a noble metal catalyst to promote hydrogenation under low hydrogen pressure, formaldehyde was not hydrogenated, but instead it could further react with 4-methylsyringol (**6**) to form homosyringaldehyde (**7**). On the other hand, it was reported by Van den Bosch, *et al.*[37] that coniferyl alcohol (**3**) reacted further to 4-n-propanol guaiacol (**8**) over Ru/C. In the current work, dihydroconiferyl alcohol (**9**) was formed over Pd/$NbOPO_4$, while isoeugenol (**10**) was formed over highly acidic catalyst Fe-H-Beta-150 (**III**). It can also be observed that in case of a low amount of catalyst (100 mg) breaking of 4-propenylsyringol (**5**) was a minor reaction, while with a high amount of catalyst (250 mg and 750 mg), 4-propenylsyringol (**5**) was rapidly dealkylated into 4-methyl syringol (**6**) and further forming homosyringaldehyde (**7**). Thus, with higher catalyst amounts, the unsaturated alcohols are unstable. Typically, the unsaturated propenyl phenol disappears quickly from the liquid phase under high hydrogen pressure[39] and the formed product is saturated propanol syringol.[37] Furthermore, 4-methyl sinapate formed *via* esterification of sinapyl alcohol (**2**).

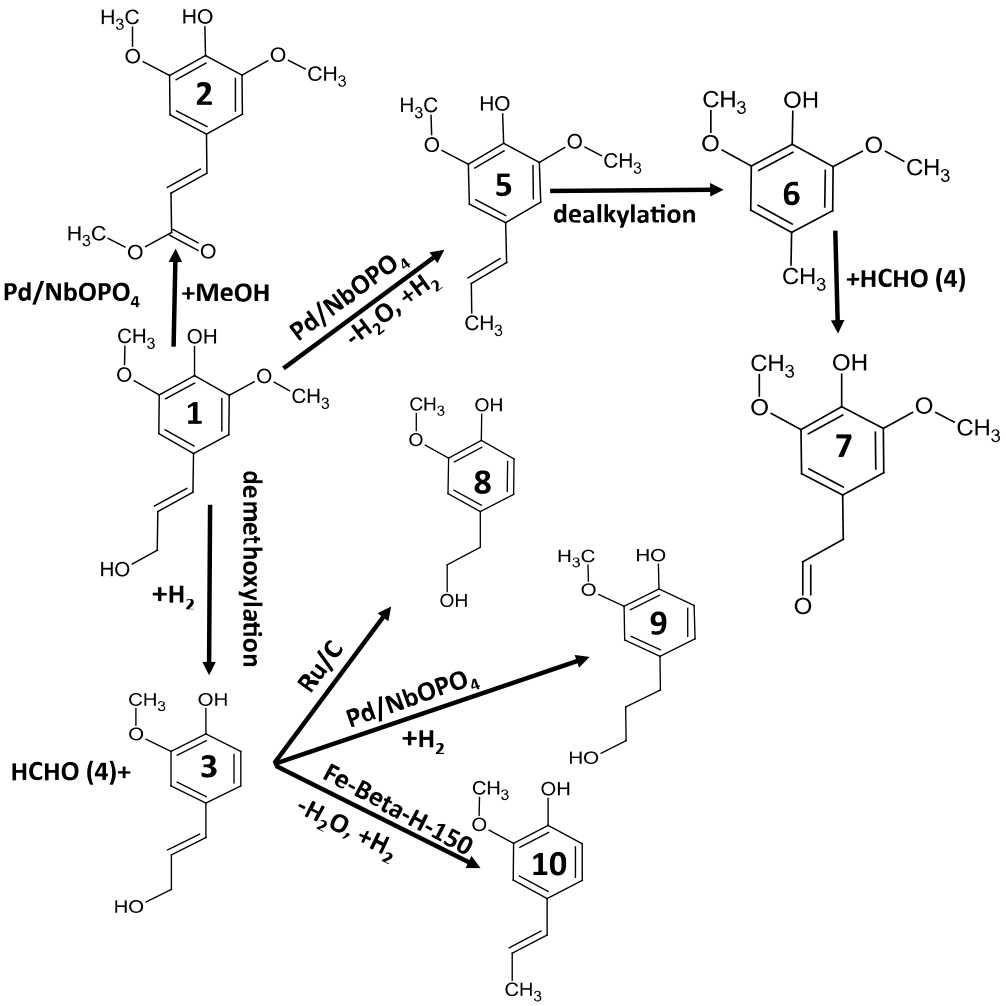

Scheme 3: The formation of main products from lignin degradation products: **1**) sinapyl alcohol, **2**) methyl sinapate, **3**) coniferyl alcohol, **4**) formaldehyde, **5**) 4-propenyl syringol, **6**) 4-methyl syringol, **7**) homosyringaldehyde, **8**) 4-*n*-propanolguaiacol, **9**) dihydroconiferyl alcohol, **10**) isoeugenol. When compared with previous studies, it can be stated that Ru/C catalysed hydrogenation forming 4-*n*-propanolguaicol (**8**) (Van den Bosch *et al.),*[39] and Fe-Beta-H-150 promoted dehydration resulting in isoeugenol (**10**) as the main compound (**III**). In the current work Pd/NbOPO4 gave homosyringaldehyde (**7**) which was formed from sinapyl alcohol (**1.**) 4-propenyl syringol (**5**) formed via dehydration from sinapyl alcohol. Dihydroconiferyl alcohol (**9**) can be formed over Pd/NbP via hydrogenation of coniferyl alcohol.

Dissolution of carbohydrates from wood, with a low amount of catalyst, 100 mg, gave 25.4 wt. % total dissolution of carbohydrates and 7.6 wt. % yield of monomeric sugars (C_5 and C_6) (**V**). The low catalyst amount did not enhance the depolymerisation to C_6 sugars. When an increased catalyst amount (250 mg) was applied, cellulose and hemicellulose dissolution efficiency was enhanced to 32 wt. %, 85 wt. %, respectively,

resulting in 14.4 wt. % sugar yield (Table 9, entry 4). In this case also the depolymerisation of hemicelluloses occurred efficiently. With 750 mg of catalyst, 8.9 wt. % of sugars was obtained (Table 9, (**V**)). It can be concluded that 250 mg of catalyst is an optimal amount for further processing. The obtained sugars comprised of high amounts of C_6 and C_5 sugars. C_6 sugars are well protected in the crystalline cellulose structure, while amorphous hemicellulose contains C_5 sugars such as xylose from xylan can be efficiently hydrolysed. The obtained sugar products can be used by for example detergent and soap industries.[72]

The optimization of reaction time results indicated that 6 h was an acceptable time to enhance lignin monomer yields up to 46 wt. % and the obtained results are close to the theoretical maximal yield of lignin monomers (Table 9, (**V**)).[39] The fractionation of wood for 12 h gave a lower aromatic yield (**V**). Analogous results were obtained by Van den Bosch *et al*.[39] It can be concluded that 6 h fractionation was the best one giving the highest amount of aromatic products. When increasing the reaction time from 3 h to 6 h with fresh wood, the total lignin monomers yield increased from 34 wt. % to 46 wt. %, and the product contains 90.2 wt. % of dimethoxyphenols and 9.8 wt. % of guaiacol related monomers (Table 9, Trial-11).

Table 9. The results from the fresh and spent wood analysis after fractionation **(V).**

Entry no.	Fresh and spent wood	Cellulose (wt. %)	Hemi cellulose (wt. %)	Klason lignin (wt. %)	Cellulose to hemi-cellulose ratio (wt. %)	Total wood dissolution (wt. %)	Delignification efficiency (wt. %)	Lignin monomer yield (%)
1	Fresh wood	43	25	25	1.7	--	--	--
2	Extractives removed wood	41	27	25	1.5	--	--	--
3	[a] Trial-3 (100 mg)	56	21	13	2.7	33	65	19
4	[a] Trial-4 (250 mg)	68	15	8	4.5	49	84	34
5	[a] Trial-6 (750 mg)	74	12	4	6.2	59	93	23
6	[b] Trial-7 (150 rpm)	66	16	6	4.1	43	86	39
7	[b] Trial-4 (300 rpm)	68	15	8	4.5	49	84	34
8	[b] Trial-8 (600 rpm)	68	17	5	4	45	89	35
9	[c] Trial-9	65	8	9	8.1	51	82	35
10	[d] Trial-10	58	16	9	3.6	40	78	9
11	[e] Trial-11	65	13	7	5	50	86	46
12	[f] Trial-12	73	7	9	10.4	60	82	41

[a] catalyst amount varied, reaction conditions: 3 h run time, and catalyst $Pd/NbOPO_4$. [b] stirring speed was varied, reaction conditions: 3 h run time, and catalyst 250 mg of $Pd/NbOPO_4$. [c] Acetone extracted wood treated with 250 mg $Pd/NbOPO_4$, 300 rpm, and 3 h run time. [d] 250 mg of $NbOPO_4$ support, 300 rpm and 3 h run time. [e] Optimum run for 6 h: 300 rpm, 250 mg of $Pd/NbOPO_4$. [f] Long run for 12 h: 300 rpm, 250 mg of $Pd/NbOPO_4$. In all experiments, 4 g of fresh wood (dry-base, ≤ 250µm) in 100 ml ethanol at 243 °C was applied. Catalyst mass or stirring speed are the studied parenthesis.

3.5.2. Catalytic liquefaction of extracted birch (**V**)

Catalytic liquefaction was performed with extracted birch over $Pd/NbOPO_4$ in supercritical ethanol under 5 bar initial hydrogen (room temperature) for 3 h and the obtained results from the spent wood indicate that the efficiency of dissolution was only slightly increased (51 wt. %) (Table 9, Trial-9, (**V**)) when related to the results from fresh wood treated with $Pd/NbOPO_4$ (Trial-4) (49 wt. %). The delignification efficiency of the extracted wood marginally decreased (82 wt. %) when related to the fresh wood (Trial-4). These results are explained due to lignin condensation during fractionation. In contrast, the yield of lignin monomers was 35 wt. % which was close to the one obtained with the fresh wood (Trial-4) and the obtained monomers comprised 93.2 wt. % of dimethoxyphenols and 6.8 wt. % of guaiacol related monomers. The main products were homosyringaldehyde (63.6 %) and dimethoxyphenol. As a comparison, Huang *et al*.[44] performed the fractionation of extracted wood over Pd/C combined with Yb(III)-triflate catalyst (co-catalyst, Lewis acid sites) in methanol at 180 °C under 30 bar initial hydrogen for 1 h and obtained 43 wt. % of lignin monomers. The main lignin monomers were 4-n-propanolguaiacol, 4-n-propylsyringol, and 4-n-methoxy propyl syringol and their guaiacyl unit derivatives.[44] When the reaction temperature and reaction time were increased from 180 to 220 °C and 1 to 2 h, respectively, the resultant monomer yields increased from 43 to 46 wt. %.[46] The concentration of hemicellulose derived methylated sugars was also increased. It was concluded that the use of heterogeneous Pd/C improves the cleavage of ether bonds, as well as metal triflates have an ease entree into lignocellulose matrix during hydrolysis.

In the spent extracted wood sugar analysis, about 8 wt. % hemicellulose remains. Even though the low amount of cellulose was dissolved, and cellulose converted into a more crystalline form. With the aim to estimate the crystalline structure of the fresh and spent extracted wood, X-ray diffraction analysis was performed. Thereupon, three distinct peaks were identified at 14.6°, 16.5° and 22.4°, respectively, confirming the presence of cellulose I with the cellulose I planes ($\bar{1}10$, 110, and 200).[42] In the $Pd/NbOPO_4$ treated extracted wood, the XRD results revealed that the presence of an increased amount of cellulose I and, simultaneously, a strong XRD peak at $2\theta=28°$ (Fig. 16), might all be related to the diffraction of cellulose acetate with certain a degree of substitution (DS).[42] The enhanced peak of cellulose acetate with DS >1.0 shows that the amorphous material is formed, since the peak height at $2\theta=28°$ was decreased.[42] The formation of cellulose acetate occurs due to presence of ethanol in the reaction medium. At supercritical conditions, ethanol is oxidized to acetic acid, which reacts with cellulose.

$$CH_3CH_2OH + CO_2 \rightarrow CH_3COOH + HCHO \quad (6)$$

The depolymerisation of wood biomass in liquefaction process generates CO_2 as a main gas component (**III**). The dehydration of sugars forms water and in the presence of hydrogen in the reaction system reaction (eq. 6) occurs.

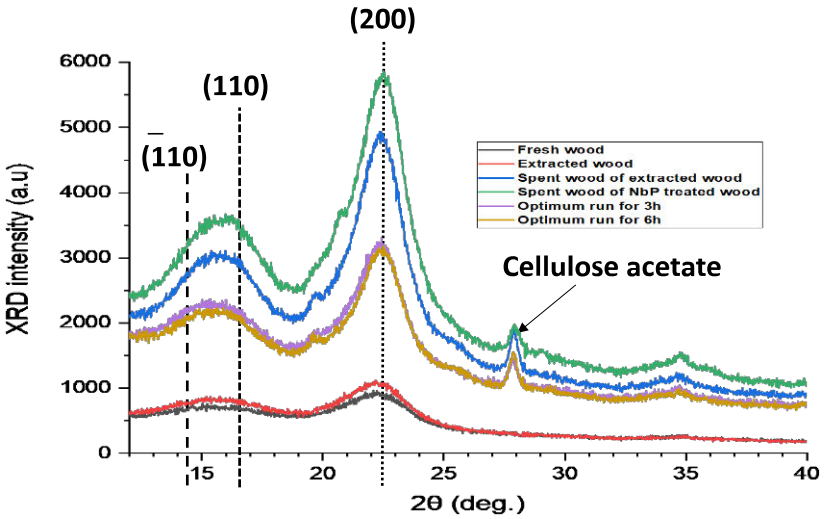

Fig 16. XRD patterns of the fresh and spent wood samples. Reaction conditions: fresh wood, extractives removed wood, spent wood of extracted wood over $Pd/NbOPO_4$ for 3 h. Spent wood of support NbP ($NbOPO_4$) treated. Optimum run, spent wood, $Pd/NbOPO_4$ treated for 3 h. Spent wood of extractives removed wood treated over $Pd/NbOPO_4$ for 6 h (**V**). In all experiments 4 g of wood (dry-base, ≤ 250 µm) in 100 ml ethanol, 300 rpm, at 243 °C was applied.

3.5.3. Influence of support and metal upon liquefaction of birch wood (**V**)

In order to determine the influence of support on depolymerisation of the fresh birch, liquefaction was performed over $NbOPO_4$ or $Pd/NbOPO_4$ in supercritical ethanol under 5 bar initial hydrogen pressure. When the reaction was performed over the $NbOPO_4$ support, the dissolution efficiency of wood was 40 wt. % and the efficiency of delignification was 78 wt. %. On the other hand, the cleavage of bonds between lignin and carbohydrates resulted only to about 9 wt. % total lignin monomers yield over $NbOPO_4$ catalyst. $NbOPO_4$ has normally a considerable amount of Brønsted acid sites (P-OH and Nb-OH) with the acidity level close to 90 % H_2SO_4 and limited portion of Lewis acid sites (Nb^{5+}).[73-74] Even the acidic properties of the $NbOPO_4$ in terms of the hydrolysis of hemicellulose, $NbOPO_4$ was ineffective for the depolymerisation of lignin and formation of monomers. This was revealed upon SEC analysis of the liquid phase samples performed after wood liquefaction. The monomers were eluting is SEC after 23 min retention time (Fig. 17). The distribution of monomers, dimers and heavy compounds, such as breaking up cellulose, hemicellulose and lignin, was also determined by SEC (Fig 17, (**V**)). The total wood fractionation capacity of the fresh wood with $NbOPO_4$ was low in the liquid product (Table 9), since a resultant in low total area of monomers was obtained in SEC chromatogram, and dimers were the major products. $NbOPO_4$ was more actively contributing to depolymerisation of the main sugar components (cellulose and hemicellulose) than lignin (Fig. 17) providing low dissolution efficiency, in spite of having a high amount of acidity (Brønsted sites). Addition of Pd to

$NbOPO_4$ enhanced depolymerisation of birch into bio-oil. Pd exhibits effective bond cleavage capability between carbohydrates and lignin such as γ-ester, phenyl ether and phenyl glycoside bonds,[46] resulting in 1.3 fold higher formation of dissolution products than formed over $NbOPO_4$ (**V**). The formed relative amounts of components over $Pd/NbOPO_4$ based on retention times in SEC chromatograms decreased as follows: dimer>monomer>heavy. Additionally, $Pd/NbOPO_4$ formed 1.5 fold more monomers than what was observed over $NbOPO_4$. The results indicated that $Pd/NbOPO_4$ is an efficient catalyst to break bonds between sugars and aromatics components and it enables the formation of high amount of monomers and dimers from lignocellulose biomass.

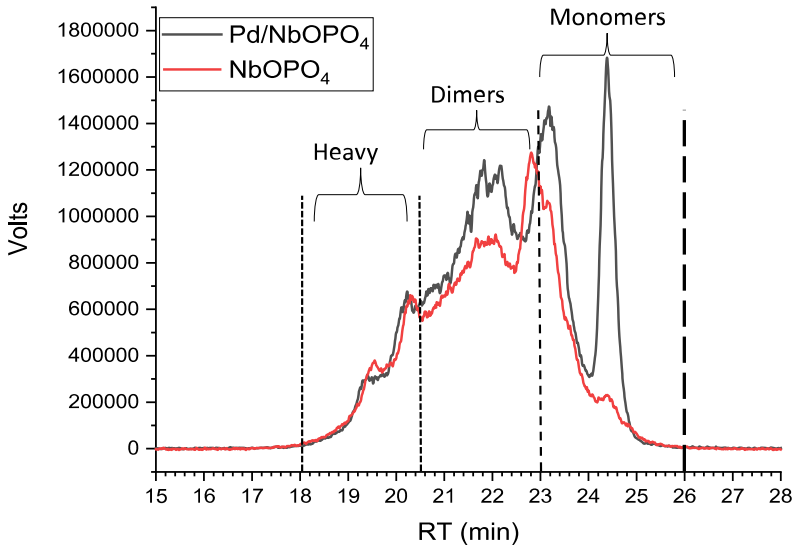

Fig 17. SEC chromatograms of fresh wood treated with $Pd/NbOPO_4$ or $NbOPO_4$ catalyst and analyzed by size exclusion chromatography (**V**).

In the current study, a limited hydrogenation activity was observed due the low applied hydrogen pressure and high temperature. Nevertheless, direct deoxygenation favored the formation of aromatic monomers, which was reported by Laskar *et al*.[75] Over a bifunctional $Pd/NbOPO_4$ catalyst, the ether bonds cleavage through hydrolysis appears over Lewis acid sites of $NbOPO_4$ and the dehydration/dealkylation of reactive intermediates was facilitated by Pd. Birch wood delignification was also demonstrated in Van den Bosch *et al*,[72] in which high amounts of phenolic monomers formed *via* syringol group breakage over Ru/C. The lignin depolymerisation *via* a tandem catalysis method occurred also over different Lewis acidic strength metal triflates along with Ru complexes.[75] The bond breaking of guaiacol-guaiacol model compound (1-(3,4-dimethoxyphenyl)-2-(2-methoxyphenoxy)ethan-l-ol) was effectively presented over $Sc(OTf)_3$ showing comparatively high amounts of Lewis acid sites (122 µmol/g). In in-

situ prepared $[Rh(cod)Cl]_2$/dppp homogeneous decarbonylation catalyst (cod: 1,5-cyclooctadiene, dppp: bis-1,3-(diphenylphosphino) propane) at 175 °C in 1,4-dioxane:water medium (9:1 v/v)[76] gave high yields of guaiacol (81 %) with enol ether hydrolysis, and a small amount of 4-methylveratrole and homoveratryl aldehyde were also formed. The aldehyde formation was suppressed by the decarbonylation catalyst. If the decarbonylation strength of the catalyst is low, high molecular weight compounds formed such as the species derived from homoveratryl aldehyde[76] and the Lewis acidic strength has the ability to control the product selectivity.[76] If the strength of Lewis acidic sites is high, the formation of decarbonylation products such as 4-methylguaiacol and 4-methylsyringol was favored.[76] Low acidic strength applied catalysts gave 4-(1-propenyl) phenols such as isoeugenol and 4-(1-propenyl) syringol. Moreover, an extracted wood depolymerisation occurred over a heterogeneous catalyst Pd/C catalyst combined with Yb(III)-metal triflates in methanol under 30 bar initial hydrogen pressure at 180 °C for 1 hr.[44] The main hydrogenated products were 4-*n*-propanolguaicol, 4-*n*-propylsyringol, 4-*n*-methoxy propyl syringol and derivatives of guaiacol units. When the reaction temperature and time increases from 180 to 220 °C, 1 h to 2 h, the yield of aromatic monomers increased from 43 wt. % to 46 wt. %.[44] Furthermore, depolymerisation studies of organosolv lignin, extracted from poplar wood was performed over heterogeneous Ni/Cu-HTC (hydrotalicite) catalyst in supercritical ethanol.[77] The main products were homosyringaldehyde (44-56 %) and guaiacylacetone (15-20 %). Under alkaline conditions, these products can undertake repolymerisation, which leads to the formation of a minor amount of aromatics.[77]

In the current study, comparatively low Lewis acidity and deoxygenation strength of the Pd/$NbOPO_4$ catalyst are the controlling features (120 µmol mixture of weak and medium Lewis acid sites) when applied in the liquefaction of the fresh birch during 3 h reaction time and, thus, 34 wt. % of lignin monomers were formed (Table 9, Trial-4). From the obtained total lignin monomers, 76.9 wt. % of dimethoxyphenols such as syringol related monomers and 16.5 wt. % of guaiacol related monomers were formed. Remarkably, the results indicated that 76.9 wt. % of dimethoxyphenol contains 61.9 wt. % of homosyringaldehyde, which was the major compound alongside with 4-propenylsyringol and 4-methylsyringol. Additionally, only a small amount of syringol was formed. Homosyringaldehyde formation in the current work can be correlated to the homoveratryl aldehyde formation upon fractionation of guaiacol-guaiacol model compound[76] or alternatively through the reaction between 4-*n*-propenyl syringol and formaldehyde. By the application of Pd/$NbOPO_4$ with relatively low Lewis acidity and dehydration strength under low hydrogen pressure and high temperature enhanced monomer formation. A considerable amount of dihydroconiferyl alcohol was also emerging over the Pd/$NbOPO_4$ catalyst.

As a comparison, when applying 5 wt. % Fe-H-Beta-150 catalyst to liquefaction of birch under low hydrogen in supercritical ethanol, isoeugenol was the main product (**IV**). Furthermore, coniferyl and 4-propenyl alcohol also formed under similar

conditions (**IV**). Under these reaction conditions, the hydrogenation capacity of Fe was low, and isoeugenol formation occurred *via* demethoxylation and dehydration reactions (**IV**). Bifunctional Pd/$NbOPO_4$ with somewhat low Lewis acidity strength, dehydration/dealkylation capacity under low hydrogen pressure and high temperature increased the phenolic monomer formation. In addition, it was stated by Lohr *et al.*[78] that the combination of weaker Lewis acid triflates $La(OTf)_3$ and Pd/C resulted in a high yield of monomers (39 %), in the acetylated dimer fractionation in dichloroethane with 30 bar H_2 at 140 °C. The acidity of the catalyst enhances hydrogenolysis, and Pd gave rise to a high hydrogenation performance directing to a better monomer yield. Furthermore, a minor amount of dimethoxyphenols were formed *via* breakage of acetylated dimers.[78] In the case of fractionation of acetone extracted wood over Pd/$NbOPO_4$, 93.2 wt. % of dimethoxyphenols and 6.8 wt. % of guaiacol related monomers were forming confirming that removal of lipophilic extractives enhanced dehydration/dealkylation (Table 9, Trial-9).

3.6. Extraction of bio-aromatic fraction with Deep Eutectic Solvent (DES) (V)

The bio-oil contains different aromatic compounds with very similar molecular structure. Furthermore, these aromatic compounds have also quite similar physical properties, for example, pKa value, solubility and boiling point. As stated in the updated open literature, the aromatic extraction from the bio-oil is typically carried out by a liquid-liquid extraction process, for instance with ethyl acetate-water,[38] ethyl ether-water[79] and dichloromethane (DCM)-water.[37,39,72] However, when using non-polar-polar solvents in the extraction step, acids and aldehydes are transferring into the non-polar organic phase beside with targeted aromatic products. A different method comprises precipitation of aromatic fraction extraction from bio-oil by addition of 0.5 M NaOH to precipitate the aromatic fraction as phenolates (salts).[79] When using non-polar solvents and acidifying the extraction medium with HCl, the following solvents, *e.g.* methyl isobutyl ketone (MIBK), dichloromethane (DCM), methyl tert-butyl ether (MTBE), toluene or isopropanol have been studied as a medium for aromatic extraction.[80-84] The main disadvantage of this extraction process is the formation of uncontrolled rigorous salts. These difficulties can be overwhelmed by using a group of "ionic liquids", such as deep eutectic solvents (DESs) in the extraction process. The nature of aromatic fraction in bio-oil has a weak Lewis acidic character with small dissociation constants. The hydrophilicity of aromatics is strengthened in the DES medium, even limiting solubilities of aromatics in aqueous phase; these characteristics can improve the extraction process.

In order to find an efficient DES for extraction of bio-aromatics from bio-crude, different DESs have been applied in the current work in bio-aromatics extraction. For instance, choline chloride based hydrogen bond donor with ester based hydrogen bond

accepter, *i.e.* ethylene glycol. The DES, ChCl: EtGly with the molar ratio of 1:4 molar has a weak acid nature (pH: 6.12).

Initially, the previously analyzed bio-oil containing ethanol extract was taken into a round bottom flasks and ethanol was removed in a rotary evaporator. The obtained bio-oil contains 54.6 wt. % of aromatics and 45.4 wt. % of other than aromatics. The whole extraction process was performed as depicted in Fig. 2. After the final steps in extraction process, a non-polar solvent, MIBK with aromatic fractions, steps (**3**+**5**, Fig. 2) contains 96 wt. % aromatic fraction and a small fraction of other than aromatics (4 wt. %). The initial ratio between aromatic fraction and other than aromatic components was equal to one. However, after extraction of the aromatic fraction, the aromatic compounds migrate from **6** to **5** (Fig. 2) with an increased rate. The whole amount of the obtained aromatic fraction (**3**+**5**, Fig. 2) contains 15.6 wt. % of heavy components, 51.2 wt. % of dimers and 33.1 wt. % of monomers, based on the SEC determination (Fig. 18). The analysis of the results aromatic fraction by GC, shows that the main components were monomers and dimers (**V**). It must be noticed that the analysis of aromatic fraction (**5**, Fig. 2) by GC detects only monomers and, a part of dimers. The outcomes indicate that in the intended extraction process (Fig. 2), DES-non-polar solvent-anti-solvent enabled extraction of the aromatic fraction from biocrude extremely well. It can, however, be stated that additional experiments are needed in order to optimize this new extraction process. The extracted aromatic components can be used in different industrial applications, for example as aviation fuel components and in polymer synthesis, etc.

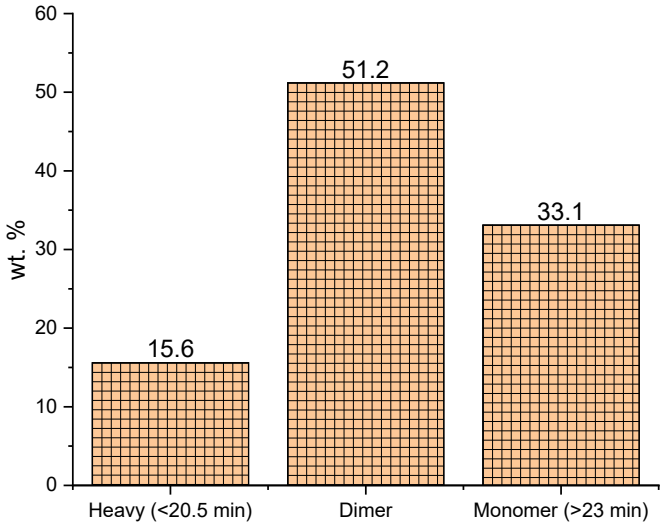

Fig 18. The SEC results of total aqueous phase extracted aromatics, and non-polar biocrude extracted aromatic fraction.

4. Conclusions and future outlook

In order to produce the needed amount of aviation fuel range cycloalkanes from lignocellulose biomass in the future, new production methods must be developed. The current work emphasized on the production of biocrude through hydrothermal liquefaction (HTL) of wood biomass over heterogeneous catalysts (5 wt. % Fe-H-Beta-150, 5 wt. % Fe-SiO_2, Pd/$NbOPO_4$ or $NbOPO_4$) containing weak and medium Brønsted and Lewis acid sites or weak Lewis acid sites under low hydrogen initial pressures. Aromatic fractions were also extracted from the obtained biocrude by applying an eco-friendly extraction method. The method includes extraction with stepwise process by choline chloride: ethylene glycol (1:4 mol) based deep eutectic solvent (DES), methyl isobutyl ketone (MIBK), and water. The resulted aromatic fraction can be further processed into cyclic hydrocarbons with high density through hydrodeoxygenation (HDO).

Hydrothermal liquefaction of birch over 5 wt. % Fe-H-Beta-150 catalyst (containing weak and medium Brønsted-Lewis acid sites) resulted in a high amount of biocrude about 25 wt. %, while in case of a non-acidic catalyst, 5 wt. % Fe-SiO_2 low biocrude yield (17 wt. %) was achieved. The resulted solid, liquid and gaseous products were fully characterized. The conversion of amorphous cellulose to crystalline form, during liquefaction of birch over 5 wt. % Fe-H-Beta-150 catalyst, was confirmed by powder X-ray diffraction analysis. The results from liquid phase analysis of birch dissolution over 5 wt. % Fe-H-Beta-150, especially upon lignin degradation, revealed that the main liquid product was isoeugenol, which is formed *via* dehydration and demethoxylation reactions. A complete reaction mechanism was proposed based on liquid phase analysis of lignin degradation products as a function of time and it was supported by a thermodynamic analysis performed with Joback approach and using Gibbs-Helmholtz equation. The amount of leached iron content in liquid phase was minor. The gaseous products comprise of low quantities of CO_2, methane, ethane, propane, and iso-butane.

In addition to Fe-based catalysts, also, Nb-based catalysts, Pd/$NbOPO_4$ (weak Lewis acid) was prepared *via* a wet impregnation method, characterized and was investigated in liquefaction of birch. In order to estimate the performance of the catalyst upon liquefaction of wood, the reaction conditions were optimized and experiments were performed both with fresh and acetone extracted birch. The resulted solid and liquid phases were comprehensively characterized with various analytical techniques. The results revealed that in birch dissolution over Pd/$NbOPO_4$, the main lignin degradation product was homosyringaldehyde, while 4-propenylsyringol, dihydroconiferyl alcohol and 4-methylsyringol were also identified. The fresh treated wood resulted in 84 wt. % delignification efficiency and the liquid phase contained 34 wt. % of phenolic monomers (composed of 76.9 wt. % of dimethoxyphenols and 16.5 wt. % of guaiacol based monomers), while the treated extracted wood gave with 78 wt. % of

delignification efficiency and the liquid phase contained 35 wt. % of phenolic monomers (93.2 wt. % of dimethoxyphenols and 6.8 wt. % of guaiacol related monomers). A plausible reaction mechanism was proposed and compared with the one obtained for Fe-based catalyst. The effect of niobium oxyphosphate support and metal upon liquefaction of birch was also discussed. From the obtained results, it can be concluded that the depolymerisation of birch occurred *via* breaking of ether bonds in lignin, including ether hydrolysis by Lewis acid sites over the solid acid catalyst and with subsequent dehydration/dealkylation of reaction intermediates by the palladium metal.

In addition, the extraction of aromatic fraction from the biocrude by a novel and eco-friendly extraction process was introduced. In the extraction process, choline chloride: ethylene glycol based (1:4 mol) deep eutectic solvent (DES) was used and further step wise addition of methyl isobutyl ketone (MIBK) and water was applied to attain maximum extraction efficiency. Finally, MIBK-phase comprising of 96 wt. % aromatic compounds, from all dissolved components, was attained.

From the whole results, it was concluded that an acidic, 5 wt. % Fe-H-Beta-150 catalyst was the better catalyst when compared with a non-acidic 5 wt. % Fe-SiO_2 catalyst. The main phenolic product is isoeugenol. However, a high amount of catalyst mass (1 g containing weak and medium Brønsted-Lewis acid sites) was required in order to attain the required compound under low hydrogen pressures. In the case of Nb-based catalysts, Pd/$NbOPO_4$ with only weak Lewis acid sites was more active and gave homosyringaldehyde as the major product. Further studies need to be carried out to the assess catalyst separation techniques and catalyst reusability. In addition, based on the current results, it is proposed more research especially in the optimization of extraction method and hydrodeoxygenation of the aromatic fraction.

5. Acknowledgements

This work was carried out between 2017 to 2021 at the Laboratory of Industrial Chemistry and Reaction Engineering, Faculty of Science and Engineering, Åbo Akademi University. The doctoral studies were a part of the activities at Johan Gadolin Process Chemistry Centre (PCC), a centre of excellence financed by Åbo Akademi. I am very glad to have the major financial support to my work from **Fortum-Neste Säätiö**, (Grant numbers 201700071, period: 2017/9-2018/8; 201800025, period: 2018/10-2019/9; 20190066, period: 2019/10-2020/8; 20200013, period: 2020/10-2021/3) and **Alfred Kordelinin Säätiö** supported preparation of dissertation (Grant number: 200207).

FORTUMIN JA NESTEEN SÄÄTIÖ

FORTUM AND NESTE FOUNDATION

Promoting energy competence – with the objective to support industry and commerce

ALFRED KORDELIN FOUNDATION

6. References

1. Change, C. (2016). What climate change. https://www.epa.gov/sites/production/files/2016-08/documents/climate_indicators_2016.pdf. Accessed August 2016.
2. Gutiérrez-Antonio, C., Gómez-Castro, F. I., de Lira-Flores, J. A., and Hernández, S. A review on the production processes of renewable jet fuel. *Renewable and Sustainable Energy Reviews* 79 (2017): 709–729.
3. International Energy Agency. (2011). Technology roadmap: biofuels for transport. Paris: IEA.
4. EIA. Biofuels issues and trends: U.S. Energy Information Administration (2012).
5. Dorrington, G. E. (2016). Certification and Performance: What Is Needed from an Aviation Fuel? In Biofuels for Aviation (pp. 35–44). Academic Press, London.
6. Zhang, X., Lei, H., Zhu, L., Wu, J., and Chen, S. From lignocellulosic biomass to renewable cycloalkanes for jet fuels. *Green Chemistry*, 17(2015), 4736–4747.
7. Kalnes, T. N., McCall, M. M., and Shonnard, D. R. Renewable diesel and jet-fuel production from fats and oils. Thermochemical conversion of biomass to liquid fuels and chemicals, *Energy and Environment Series* 1 (2010): 468–495.
8. Yang, X., Li, T., Tang, K., Zhou, X., Lu, M., Ounkham, W. L., Spain, S. M., Frost, B. J., and Lin, H. Highly efficient conversion of terpenoid biomass to jet-fuel range cycloalkanes in a biphasic tandem catalytic process. *Green Chemistry*, 19, 15 (2017): 3566–3573.
9. Morgan, T., Santillan-Jimenez, E., Harman-Ware, A. E., Ji, Y., Grubb, D., and Crocker, M. Catalytic deoxygenation of triglycerides to hydrocarbons over supported nickel catalysts. *Chemical Engineering Journal* 189 (2012): 346–355.
10. Yuhan, Y., Wang, Q., Zhang, X., Wang, L and Li, G. Hydrotreating of C_{18} fatty acids to hydrocarbons on sulphided $NiW/SiO_2–Al_2O_3$. *Fuel Processing Technology* 116 (2013): 165–174.
11. Wei, H., Liu, W., Chen, X., Yang, Q., Li, J., and Chen, H. Renewable bio-jet fuel production for aviation: A review. *Fuel* 254 (2019): 115599.
12. Albersheim, P., Darvill, A., Roberts, K., Sederoff, R., and Staehelin, A. (2010). *Plant cell walls*. Garland Science.
13. van Dyk, S., Saddler, J., Boshell, F., Saygin, D., Salgado, A., and Seleem, A. (2017). Biofuels for aviation: technology brief. International Renewable Energy Agency, Abu Dhabi.
14. Tung, C. C., and Jo-Han, N. A review of biomass gasification technology to produce syngas. *American-Eurasian Journal of Sustainable Agriculture* (2014): 69–75.
15. Li, X. T., Grace, J. R., Lim, C. J., Watkinson, A. P., Chen, H. P and Kim, J. R. Biomass gasification in a circulating fluidized bed. *Biomass and bioenergy* 26, 2 (2004): 171–193.
16. Basu, P (2010) Biomass Gasification and Pyrolysis: Practical Design and Theory. Burlington, MA: Elsevier.
17. Di Blasi, C. Modeling chemical and physical processes of wood and biomass pyrolysis. *Progress in Energy and Combustion Science* 34, 1 (2008): 47–90.
18. Kwiatkowski, K., Bajer, K., Celińska, A., Dudyński, M., Korotko, J., and Sosnowska, M. Pyrolysis and gasification of a thermally thick wood particle-Effect of fragmentation. *Fuel* 132 (2014): 125–134.
19. Dai, J., Saayman, J., Grace, J. R., and Ellis, N. Gasification of woody biomass. *Annual review of Chemical and Biomolecular Engineering* 6 (2015): 77–99.

20. Williams, R. H., Larson, E. D., Liu, G., and Kreutz, T. G. Fischer–Tropsch fuels from coal and biomass: Strategic advantages of once-through ("polygeneration") configurations. *Energy Procedia* 1, 1 (2009): 4379–4386.

21. Bridgwater, A. V. Review of fast pyrolysis of biomass and product upgrading. *Biomass and Bioenergy* 38 (2012): 68-94.

22. Horne, P. A., & Williams, P. T. Influence of temperature on the products from the flash pyrolysis of biomass. *Fuel* 75, 9 (1996): 1051–1059.

23. Scott, D. S., Piskorz, J., and Radlein, D. Liquid products from the continuous flash pyrolysis of biomass. *Industrial & Engineering Chemistry Process Design and Development* 24, 3 (1985): 581–588.

24. Radlein, D., and Quignard, A. A short historical review of fast pyrolysis of biomass. *Oil & Gas Science and Technology–Revue d'IFP Energies nouvelles* 68, 4 (2013): 765–783.

25. Wei, H., Liu, W., Chen, X., Yang, Q., Li, J., and Chen, H. Renewable bio-jet fuel production for aviation: A review. *Fuel* 254 (2019): 115599.

26. Sutton, A. D., Waldie, F. D., Wu, R., Schlaf, M., Louis, A., & Gordon, J. C. The hydrodeoxygenation of bioderived furans into alkanes. *Nature Chemistry* 5, 5 (2013): 428–432.

27. Li, G., Li, N., Yang, J., Wang, A., Wang, X., Cong, Y., and Zhang, T. Synthesis of renewable diesel with the 2-methylfuran, butanal and acetone derived from lignocellulose. *Bioresource Technology* 134 (2013): 66–72.

28. Harvey, B. G., Wright, M. E., and Quintana, R. L. High-density renewable fuels based on the selective dimerization of pinenes. *Energy & Fuels* 24, 1 (2010): 267-273.

29. Bruno, T. J., Bruno, T. J., Huber, M. L., Laesecke, A., Lemmon, E. W., and Perkins, R. A. Thermochemical and thermophysical properties of JP-10. (2006): 325.

30. Meylemans, H. A., Quintana, R. L., and Harvey, B. G. Efficient conversion of pure and mixed terpene feedstocks to high density fuels. *Fuel* 97 (2012): 560–568.

31. Mobile, Exxon. World jet fuel specification. Leatherhead (UK): Exxon Mobile (2005).

32. Chung, H. S., Chen, C. S. H., Kremer, R. A., Boulton, J. R., and Burdette, G. W. Recent developments in high-energy density liquid hydrocarbon fuels. *Energy & Fuels* 13, 3 (1999): 641–649.

33. Zhao, C., He, J., Lemonidou, A. A., Li, X., and Lercher, J. A. Aqueous-phase hydrodeoxygenation of bio-derived phenols to cycloalkanes. *Journal of Catalysis* 280, 1 (2011): 8–16.

34. Yang, Y., Du, Z., Huang, Y., Lu, F., Wang, F., Gao. J., and Xu, J., Conversion of furfural into cyclopentanone over Ni–Cu bimetallic catalysts. *Green Chemistry* 15, 7 (2013): 1932–1940.

35. Yang, J., Li, N., Li, G., Wang, W., Wang, A., Wang, X., Cong, Y., and Zhang, T., Synthesis of renewable high-density fuels using cyclopentanone derived from lignocellulose. *Chemical Communications* 50, 20 (2014): 2572–2574.

36. Matsumura, Y., Nonaka, H., Yokura, H., Tsutsumi, A., and Yoshida, K. Co-liquefaction of coal and cellulose in supercritical water. *Fuel* 78, 9 (1999): 1049–1056.

37. Van den Bosch, S., Schutyser, W., Koelewijn, S-F., Renders, T., Courtin, C. M., and Sels, B. F. Tuning the lignin oil OH-content with Ru and Pd catalysts during lignin hydrogenolysis on birch wood. *Chemical Communications* 51, 67 (2015): 13158–13161.

38. Ouyang, X., Huang, X., Zhu, J., Boot, M. D., and Hensen, E. J. Catalytic conversion of lignin in woody biomass into phenolic monomers in methanol/water mixtures without external hydrogen. *ACS Sustainable Chemistry & Engineering* 7, 16 (2019): 13764–13773.

39. Van den Bosch, S., Renders, T., Kennis, S., Koelewijn, S.-F., Van den Bossche, G., Vangeel, T., Deneyer, A., Depuydt, D., Courtin, C. M., Thevelein, J. M., Schutyser W., and Sels, B. F. Integrating lignin valorization and bio-ethanol production: on the role of Ni-Al_2O_3 catalyst pellets during lignin-first fractionation. *Green Chemistry* 19, 14 (2017): 3313–3326.

40. Rautiainen, S., Di Francesco, D., Katea, S. N., Westin, G., Tungasmita, D. N., and Samec, J. S. Lignin valorization by cobalt-catalyzed fractionation of lignocellulose to yield monophenolic compounds. *ChemSusChem* 12, 2 (2019): 404–408.

41. Araya, P. E., Droguett, S. E., Neuburg, H. J., and Badilla-Ohlbaum, R. Catalytic wood liquefaction using a hydrogen donor solvent. *The Canadian Journal of Chemical Engineering* 64, 5 (1986): 775–780.

42. Xu, C., and Etcheverry, T. Hydro-liquefaction of woody biomass in sub-and super-critical ethanol with iron-based catalysts. *Fuel* 87, 3 (2008): 335–345.

43. Beauchet, R., Pinard, L., Kpogbemabou, D., Laduranty, J., Lemee, L., Lemberton, J.L., Bataille, F., Magnoux, P., Ambles, A., and Barbier, J. Hydroliquefaction of green wastes to produce fuels. *Bioresource Technology* 102, 10 (2011): 6200–6207.

44. Huang, X., Zhu, J., Korányi, T. I., Boot, M. D., and Hensen, E. J. Effective release of lignin fragments from lignocellulose by Lewis acid metal triflates in the lignin-first approach. *ChemSusChem* 9, 23 (2016): 3262–3267.

45. Zhang, X., Tang, W., Zhang, Q., Wang, T., and Ma, L. Hydrodeoxygenation of lignin-derived phenoic compounds to hydrocarbon fuel over supported Ni-based catalysts. *Applied Energy* 227 (2018): 73–79.

46. Samikannu, A., Konwar, L. J., Rajendran, K., Lee, C. C., Shchukarev, A., Virtanen, P., and Mikkola, J. P. Highly dispersed $NbOPO_4$/SBA-15 as a versatile acid catalyst upon production of renewable jet-fuel from bio-based furanics via hydroxyalkylation-alkylation (HAA) and hydrodeoxygenation (HDO) reactions. *Applied Catalysis B: Environmental* (2020): 118987.

47. Fang, Q., Jiang, Z., Guo, K., Liu, X., Li, Z., Li, G., and Hu, C. Low temperature catalytic conversion of oligomers derived from lignin in pubescens on Pd/$NbOPO_4$. *Applied Catalysis B: Environmental* 263 (2020): 118325.

48. Emeis, C. A. Determination of integrated molar extinction coefficients for infrared absorption bands of pyridine adsorbed on solid acid catalysts. *Journal of Catalysis* 141, 2 (1993): 347–354.

49. Jablonsky, M., Vernarecová, M., Ház, A., Dubinyová, L., Skulcova, A., Sladková, A., and Surina, I. Extraction of phenolic and lipophilic compounds from spruce (*Picea abies*) bark using accelerated solvent extraction by ethanol. *Wood Research* 60, 4 (2015): 583–590.

50. Vucetic, N., Virtanen, P., Nuri, A., Mattson, I., Aho, A., Mikkola, J.-P. and Salmi, T. Preparation and characterization of a new bis-layered supported ionic liquid catalyst (SILCA) with an unprecedented activity in the Heck reaction. *Journal of Catalysis* 371 (2019): 35–46.

51. Rogošić, M., and Kučan, K. Z. Deep eutectic solvents based on choline chloride and ethylene glycol as media for extractive denitrification/desulfurization/dearomatization of motor fuels. *Journal of Industrial and Engineering Chemistry* 72 (2019): 87–99.

52. Santoni, I., Callone, E., Sandak, A., Sandak, J., and Dirè, S. Solid state NMR and IR characterization of wood polymer structure in relation to tree provenance. *Carbohydrate Polymers* 117 (2015): 710–721.

53. Huang, X., Atay, C., Zhu, J., Palstra, S. W., Korányi, T. I., Boot, M. D., and Hensen, E. J. Catalytic depolymerization of lignin and woody biomass in supercritical ethanol: influence of reaction temperature and feedstock. *ACS Sustainable Chemistry & Engineering* 5, 11 (2017): 10864–10874.

54. Anderson, E. M., Katahira, R., Reed, M., Resch, M. G., Karp, E. M., Beckham, G. T., and Román-Leshkov, Y. Reductive catalytic fractionation of corn stover lignin. *ACS Sustainable Chemistry & Engineering* 4, 12 (2016): 6940–6950.

55. Comisar, C. M., Hunter, S. E., Walton, A., and Savage, P. E. Effect of pH on ether, ester, and carbonate hydrolysis in high-temperature water. *Industrial & Engineering Chemistry Research* 47, 3 (2008): 577–584.

56. Higuchi, T., Tanahashi, M., and Mastukura, M. Production of 2,6-bis(4-hydroxy-3,5-dimethoxyphenyl-3, 7-dioxabicyclo (3.3. 0) octane. *U.S. Patent* 4,684,740, issued August 4, 1987.

57. Zhang, J., Sun, J., Sudduth, B., Hernandez, X. P., and Wang, Y. Liquid-phase hydrodeoxygenation of lignin-derived phenolics on Pd/Fe: A mechanistic study. *Catalysis Today* 339 (2020): 305–311.

58. Prasomsri, T., Shetty, M., Murugappan, K., and Román-Leshkov, Y. Insights into the catalytic activity and surface modification of MoO_3 during the hydrodeoxygenation of lignin-derived model compounds into aromatic hydrocarbons under low hydrogen pressures. *Energy & Environmental Science* 7, 8 (2014): 2660–2669.

59. Lee, W. S., Wang, Z., Wu, R. J., and Bhan, A. Selective vapor-phase hydrodeoxygenation of anisole to benzene on molybdenum carbide catalysts. *Journal of Catalysis* 319 (2014): 44–53.

60. Huang, X., Gonzalez, O. M. M., Zhu, J., Korányi, T. I., Boot, M. D., and Hensen, E. J. Reductive fractionation of woody biomass into lignin monomers and cellulose by tandem metal triflate and Pd/C catalysis. *Green Chemistry* 19, 1 (2017): 175–187.

61. Wu, Z., Wang, F., Xu, J., Zhang, J., Zhao, X., Hu, L., and Jiang, Y. Improved lignin pyrolysis over attapulgite-supported solid acid catalysts. *Biomass Conversion and Biorefinery* (2020): 1–10.

62. Schutyser, W., Van den Bosch, S., Tom, R., De Boe, T., Koelewijn, S-F., Annelies, D., Thijs, E., Verkinderen, O., Goderis, B., Courtin, C. M., and Sels, B. F. Influence of bio-based solvents on the catalytic reductive fractionation of birch wood. *Green Chemistry* 17, 11 (2015): 5035–5045.

63. Cox, B. J., Jia, S., Zhang, Z. C., and Ekerdt, J. G. Catalytic degradation of lignin model compounds in acidic imidazolium based ionic liquids: Hammett acidity and anion effects. *Polymer Degradation and Stability* 96, 4 (2011): 426–431.

64. Binder, J. B., Gray, M. J., White, J. F., Zhang, Z. C., and Holladay, J. E. Reactions of lignin model compounds in ionic liquids. *Biomass and Bioenergy* 33, 9 (2009): 1122–1130.

65. Shafaghat, H., Pouya, S. R., and Wan, M. A. W. D. Catalytic hydrodeoxygenation of simulated phenolic bio-oil to cycloalkanes and aromatic hydrocarbons over bifunctional metal/acid catalysts of Ni/HBeta, Fe/HBeta and NiFe/HBeta. *Journal of Industrial and Engineering Chemistry* 35 (2016): 268–276.

66. Bomont, L., Alda-Onggar, M., Fedorov, V., Aho, A., Peltonen, J., Eränen, K., Markus, P., Kumar, N., Wärnå, J. Russo, V., Mäki-Arvela, P., Grénman, H., Lindblad, M., and Murzin, D. Y. Production of cycloalkanes in hydrodeoxygenation of isoeugenol over Pt-and Ir-modified bifunctional Catalysts. *European Journal of Inorganic Chemistry* 24 (2018): 2841–2854.

67. Alda-Onggar, M., Mäki-Arvela, P., Aho, A., Simakova, I. L. and Murzin, D. Y. Hydrodeoxygenation of phenolic model compounds over zirconia supported Ir and Ni-catalysts. *Reaction Kinetics, Mechanisms and Catalysis* 126, 2 (2019): 737–759.

68. Zemansky, M. W., Michael, M. A., and Hendrick, C. V. N. Basic engineering thermodynamics. *McGraw-Hill Companies*, 1975.

69. Bruce E. P., Prausnitz, M., and O'Connell, J. P. The Properties of Gases and Liquids. (2004). ISBN-13: 978-0070116825.

70. Joback, K. G. A unified approach to physical property estimation using multivariate statistical techniques. PhD diss., *Massachusetts Institute of Technology*, 1984.

71. Joback, K. G., and Reid, R. C. Estimation of pure-component properties from group-contributions. *Chemical Engineering Communications* 57, 1-6 (1987): 233–243.

72. Van den Bosch, S., Schutyser, W., Ruben, V., Tine, D., Koelewijn, S-F., Renders, T., De Meester, B., Huijgen, W. J. J., Dehaen, W., Courtin, C. M., Lagrain, B., Boerjan, W., and Sels, B. F. Reductive lignocellulose fractionation into soluble lignin-derived phenolic monomers and dimers and processable carbohydrate pulps. *Energy & Environmental Science* 8, 6 (2015): 1748–1763.

73. Sarkar, A., and Pramanik, P. Synthesis of mesoporous niobium oxophosphate using niobium tartrate precursor by soft templating method. *Microporous and Mesoporous materials* 117, 3 (2009): 580–585.

74. Okuhara, T. Water-tolerant solid acid catalysts. *Chemical Reviews* 102, 10 (2002): 3641–3666.

75. Laskar, D. D., Yang, B., Wang, H., and Lee, J. Pathways for biomass-derived lignin to hydrocarbon fuels. *Biofuels, Bioproducts and Biorefining* 7, 5 (2013): 602–626.

76. Jastrzebski, R., Constant, S., Lancefield, C. S., Westwood, N. J., Weckhuysen, B. M., and Bruijnincx, P. C. Tandem Catalytic Depolymerization of Lignin by Water-Tolerant Lewis Acids and Rhodium Complexes. *ChemSusChem* 9, 16 (2016): 2074.

77. Cornejo, A., Bimbela, F., Moreira, R., Hablich, K., García-Yoldi, Í., Maisterra, M., Portugal, A., Gandía, L. M., and Martínez-Merino, V. Production of aromatic compounds by catalytic depolymerization of technical and downstream biorefinery lignins. Biomolecules, 10(9) (2020), 1338.

78. Lohr, T. L., Li, Z., and Marks, T. J. Selective ether/ester C–O cleavage of an acetylated lignin model via tandem catalysis. *ACS Catalysis* 5, 11 (2015): 7004–7007.

79. Liu, Y., Chen, L., Wang, T., Zhang, Q., Wang, C., Yan, J., and Ma, L. one-pot catalytic conversion of raw lignocellulosic biomass into gasoline alkanes and chemicals over $LiTaMoO_6$ and Ru/C in aqueous phosphoric acid. *ACS Sustainable Chemistry & Engineering* 3, 8 (2015): 1745–1755.

80. Žilnik, L. F., and Jazbinšek, A. Recovery of renewable phenolic fraction from pyrolysis oil. *Separation and Purification Technology* 86 (2012): 157–170.

81. Li, J., Wang, C., and Yang, Z. Production and separation of phenols from biomass-derived bio-petroleum. *Journal of Analytical and Applied Pyrolysis* 89, 2 (2010): 218–224.

82. Mantilla, S. V., Manrique, A. M., and Gauthier-Maradei, P. Methodology for extraction of phenolic compounds of bio-oil from agricultural biomass wastes. *Waste and Biomass Valorization* 6, 3 (2015): 371–383.

83. Wang, S., Wang, Y., Cai, Q., Wang, X., Jin, H., and Luo, Z. Multi-step separation of monophenols and pyrolytic lignins from the water-insoluble phase of bio-oil. *Separation and Purification Technology* 122 (2014): 248–255.

84. Mante, O. D., Thompson, S. J., Mustapha, S., and Dayton, D. C. A selective extraction method for recovery of monofunctional methoxyphenols from biomass pyrolysis liquids. *Green Chemistry* 21, 9 (2019): 2257–2265.

ISBN 978-952-12-4039-3 (PRINTED VERSION)/ ISBN 978-952-12-4040-9 (DIGITAL VERSION)
ISSN 2669-8315 2670-0638 (ACTA TECHNOLOGIAE CHEMICAE ABOENSIA 2019 A/1)
PAINOSALAMA OY ÅBO/TURKU 2021